Bollettino della Società Paleontologica Italiana, 58 (1), 2019, 85-108. Modena

The Italian record of the Palaeocene-Eocene Thermal Maximum

Luca Giusberti, Luca Capraro, Valeria Luciani & Eliana Fornaciari

L. Giusberti, Dipartimento di Geoscienze, Università degli Studi di Padova, Via G. Gradenigo 6, I-35131 Padova; luca.giusberti@unipd.it
L. Capraro, Dipartimento di Geoscienze, Università degli Studi di Padova, Via G. Gradenigo 6, I-35131 Padova; luca.capraro@unipd.it
V. Luciani, Dipartimento di Fisica e Scienze della Terra, Via G. Saragat 1, I-44122 Ferrara; valeria.luciani@unife.it
E. Fornaciari, Dipartimento di Geoscienze, Università degli Studi di Padova, Via G. Gradenigo 6, I-35131 Padova; eliana.fornaciari@unipd.it

KEY WORDS - Early Eocene, Hyperthermal, Global warming, Italy.

ABSTRACT - The present paper summarises the state of the art of the studies on Italian Palaeocene-Eocene Thermal Maximum (PETM) records. The PETM (~ 56 Ma) likely represents the most dramatic and rapid event of global climate warming of the whole Cenozoic. During the PETM, temperatures at the Earth's surface probably increased by at least 5°C over a few thousand years, and remained thereafter exceptionally high for over 100 k.y. Hallmark of the PETM is a negative excursion in stable carbon isotopes globally recognised that is generally interpreted as the response to a massive and sudden input of isotopically light carbon into the ocean-atmosphere system, which eventually gave rise to a rapid and extreme global warming. Climatic perturbations associated with the PETM were severe and affected both the marine and terrestrial domains, triggering faunal and floral turnovers and radiations, migrations and the most dramatic Cenozoic deep-sea benthic foraminiferal extinction event. Since the beginning of the 2000s, insightful contributions to this topic have been provided by the investigations of lower Palaeogene marine Italian records from the Umbria-Marche (Northern Apennines, Italy) and Belluno (Southern Alps, Italy) basins. In particular, crucial reference sections found in Scaglia Rossa-type facies, such as the Contessa, Possagno, Forada and Cicogna sections, have significantly improved our knowledge of the biotic and abiotic events associated to the PETM. Among these, the Forada section (Belluno Basin) was the focus of accurate integrated micropalaeontological (calcareous plankton and benthic foraminifera) and geochemical-stratigraphical studies, which possibly offer the most complete reconstruction across the PETM available in Europe to date.

RIASSUNTO - [Il record italiano del Palaeocene-Eocene Thermal Maximum] - *Il Palaeocene-Eocene Thermal Maximum (PETM; ca. 56 Ma) rappresenta probabilmente il più drammatico e rapido evento di riscaldamento globale dell'intero Cenozoico. I dati disponibili suggeriscono che, durante il PETM, le temperature sulla superficie terrestre aumentarono di circa 5°C in poche migliaia di anni, rimanendo poi eccezionalmente alte per oltre 100.000 anni. Il tratto più caratteristico del PETM è rappresentato da un'ampia escursione negativa degli isotopi stabili del carbonio (la cosiddetta Carbon Isotope Excursion, CIE; 2-7‰), riconosciuta a scala globale e generalmente interpretata come la risposta a una massiccia e improvvisa immissione di carbonio isotopicamente leggero nel sistema Terra-Atmosfera. Questo fenomeno determinò, in ultima istanza, un rapido riscaldamento a scala globale che finì per portare il sistema climatico a livelli di stress senza precedenti. Le perturbazioni climatiche associate al PETM furono severe e interessarono sia il dominio marino sia quello continentale, innescando radiazioni di fauna e flora, migrazioni, e il più drammatico evento di estinzione tra i foraminiferi bentonici cenozoici di acque profonde, il cosiddetto BEE (benthic foraminiferal extinction event). Dall'inizio degli anni 2000, contributi fondamentali allo studio del PETM sono stati forniti da indagini eseguite sui record marini italiani del Paleogene inferiore affioranti nel contesto dei bacini sedimentari umbro-marchigiani (Appennino Settentrionale, Italia centrale) e bellunesi (Sudalpino orientale, Italia settentrionale). Nello specifico, sezioni in facies di Scaglia Rossa quali la Contessa, Possagno, Forada e Cicogna, hanno fornito una documentazione di cruciale importanza per lo sviluppo delle conoscenze sugli eventi associati al PETM. Tra questi, la sezione del Forada (Bacino di Belluno) è stata oggetto di accurati studi integrati con ricostruzioni di tipo micropaleontologico (plancton calcareo e foraminiferi bentonici) e geochimico-stratigrafico ad altissima risoluzione, che offrono - a nostra conoscenza - una delle più complete documentazioni del PETM attualmente disponibili in Europa.*

INTRODUCTION

The Palaeocene/Eocene boundary (~56 Ma) is marked by the most intense and dramatic climatic disruption of the entire Cenozoic, i.e., the Palaeocene-Eocene Thermal Maximum (PETM or, previously, "Late Palaeocene Thermal Maximum"; Zachos et al., 2001; Aubry et al., 2007; Sluijs et al., 2007; Mc Inerney & Wing, 2011). This short-term event of global warming ("hyperthermal" sensu Foster et al., 2018), superimposed on the late Palaeocene-early Eocene long-term warming trend, culminated in the Early Eocene Climatic Optimum (EECO; Zachos et al., 2001). The PETM was characterised by temperature increases of 4-5°C at the Earth's surface, which occurred over just a few thousand years (e.g., Mc Inerney & Wing, 2011; Dunkley Jones et al., 2018). Hallmark of the PETM, lasting between ~170 and ~230 k.y. (e.g., Röhl et al., 2007; Murphy et al., 2010), is a large negative excursion in stable carbon isotopes (the carbon isotope excursion, CIE) that is recognised worldwide both in marine and terrestrial settings (e.g., Kennett & Stott, 1990, 1991; Koch et al., 1992). Its magnitude ranges from ~2-4.5‰ in marine carbonates to 4-7‰ in marine and terrestrial organic carbon records (see Giusberti et al., 2016 and references therein) and implies a perturbation of the global carbon cycle in response to a massive and abrupt input of isotopically depleted carbon into the ocean-atmosphere system, rapidly leading to an extreme global warming (e.g., McInerney & Wing, 2011). The onset of the CIE was paralleled by a dramatic ocean acidification and shallowing of the calcite compensation depth (CCD; Zachos et al., 2005), as well as a significant increase of the terrigenous input to continental margins (e.g., Schmitz et al., 2001; Egger et al., 2005; Giusberti et al., 2007; Pujalte

ISSN 0375-7633

doi:10.4435/BSPI.2019.06

et al., 2015; Dunkley Jones et al., 2018) that resulted in major lithologic changes (carbonate dissolution intervals and siliciclastic units: CDI and SU; Coccioni et al., 1994; Schmitz et al., 2001). In spite of almost three decades of intensive investigations, disagreements persist on the source, mass and injection rate of the "light" carbon released during the PETM (e.g., Frieling et al., 2016; Gutjahr et al., 2018; Turner, 2018). Trigger mechanisms proposed so far also include, among others, variations in the Earth's orbit and extra-terrestrial impacts (De Conto et al., 2012; Schaller & Fung, 2018). Similarly, mechanisms responsible for both the climatic and isotopic recovery at the end of the PETM are still uncertain (e.g., Bowen & Zachos, 2010; Dunkley Jones et al., 2018). Major biotic turnovers are associated with the PETM, as terrestrial and marine organisms experienced large modifications in their geographic ranges, rapid evolution and changes in trophic strategies (e.g., Sluijs et al., 2007; McInerney & Wing, 2011). The best documented turnover in the marine environment is probably the extinction event of bathyal and abyssal benthic foraminifera that affected ~30-50% of deep-water species (BEE, benthic foraminiferal extinction event), thus representing the largest benthic foraminiferal extinction in the past 90 Ma (e.g., Thomas, 1998, 2007; Speijer et al., 2012; Alegret et al., 2018, and references therein). Terrestrial records of the PETM witness significant mammalian turnovers, including the sudden appearance of three modern mammalian orders (artiodactyls, perissodactyls and primates; APP taxa) as well as mammalian dwarfing in both immigrant and endemic taxa (e.g., Gingerich, 2003, 2006; D'Ambrosia et al., 2017). Overall, the biotic changes associated with PETM indicate that, from the continent to the deep ocean, the biosphere was pervasively perturbed by a rapid climate change that left a permanent mark on macroevolutionary patterns (e.g., Speijer et al., 2012). Because of the different durations and timings involved, the PETM hyperthermal cannot be considered as a direct analogue of the "Anthropocene". However, it can provide a unique set of information on the response of both the global climate system and biota to an abrupt and massive carbon addition in to the ocean-atmosphere system (Foster et al., 2018).

The role of the Tethyan area in PETM studies

The discovery of the PETM in the early 1990s (Kennett & Stott, 1990, 1991) prompted an early Palaeogene hyperthermals "saga", and henceforth, the climate and biota from lower Palaeogene records became the focus of several ODP and IODP oceanic expeditions and researches presented and discussed in dedicated congresses (e.g., CBEP: Climate and Biota of the early Palaeogene). Efforts in expanding the information across the PETM from a wide array of palaeoenvironmental settings led to the intensive exploitation of continental and on-land marine sedimentary archives.

Bathyal and shelfal successions of the Tethyan area, such as Spain, North Africa and the Middle East, became sites of extensive studies (e.g., Molina et al., 1994; Speijer, 1994; Canudo et al., 1995; Charisi & Schmitz, 1995; Lu et al., 1995; Ortiz, 1995; Angori & Monechi, 1996; Speijer et al., 1996). These investigations acknowledged that probably the Tethyan area was a massive source of warm and saline deep-waters, which might have played a critical role in driving the deep ocean warming at the P/E boundary (Kennett & Stott, 1990, 1991; Arenillas et al., 1999). Data gathered from the Tethys significantly improved the knowledge on several aspects of the "Late Palaeocene Thermal Maximum" (Zachos et al., 1993), which was still largely undocumented at that time. These efforts were paralleled and fuelled by the need for a suitable GSSP candidate for the Palaeocene/Eocene boundary. Eventually, the Dababyia section (Egypt) was ratified as the stratotype for the base of the Ypresian, with the onset of the CIE as the best criterion for recognising and correlating the boundary (Aubry et al., 2007; Gradstein et al., 2012).

Mesozoic-Palaeogene pelagic records of the Tethyan realm are well preserved and exposed in Italy, namely in the Northern Apennines (Umbria and Marche regions) and Southern Alps (Veneto region) (Fornaciari et al., 2007). Although entered into the PETM "business" later (end of the 1990s) than other Mediterranean regions (e.g., Spain, Egypt), they provided key contributions to the knowledge of the PETM as summarised below.

THE PETM RECORD IN THE UMBRIA-MARCHE BASIN (CENTRAL ITALY)

Because of its remarkable record of several crucial events of the Earth's history, spanning from the Cretaceous/Palaeogene (K/Pg) boundary to the Palaeogene/Neogene (Pg/Ng) boundary (e.g., Coccioni et al., 2012, 2013, 2016 and references therein), the Palaeogene pelagic and hemipelagic carbonate succession located in the Umbria-Marche Basin, close to the historical locality of Gubbio (Fig. 1a), is undoubtedly the most thoroughly studied record in the Tethys. The local Palaeogene succession is represented in the area by three distinct formations, namely the Scaglia Rossa (lower Turonian-middle Eocene), Scaglia Variegata (middle-upper Eocene) and Scaglia Cinerea (upper Eocene-lowermost Miocene). Such formations are composed of biogenic carbonates (ancient nanno-foraminiferal oozes) deposited well above the CCD at middle to lower bathyal depths, and at a palaeolatitude ranging from 30°N to 40°N (from K/Pg to Pg/Ng boundary; Coccioni et al., 2013, 2016).

Fig. 1 - The PETM record in the Contessa Road section. a) Location map of Contessa and Bottaccione sections (Umbria Marche Basin, central Italy; after Coccioni et al., 2016). b) Location map of some sections of the pelagic Palaeogene composite succession (PPCS), including the Contessa Road section (after Coccioni et al., 2016). c) The outcrop of the PETM record at Contessa Road with indication of the lower and upper marly beds M1 and M2. The CIE onset and the BEE fall within the lower BED M1 (courtesy of Rodolfo Coccioni). d) Simplified log and stable isotope record of the PETM at Contessa Road section (modified after Galeotti et al., 2000). e) Synopsis of bioevents recognised in the Deep Water Agglutinated Foraminifera (DWAF) across the Palaeocene/Eocene boundary at Contessa Road section. Biozonal scheme 1 after Martini (1971), 2 after Okada & Bukry (1980), 3 after Berggren et al. (1995). Redrawn from Galeotti et al. (2004).

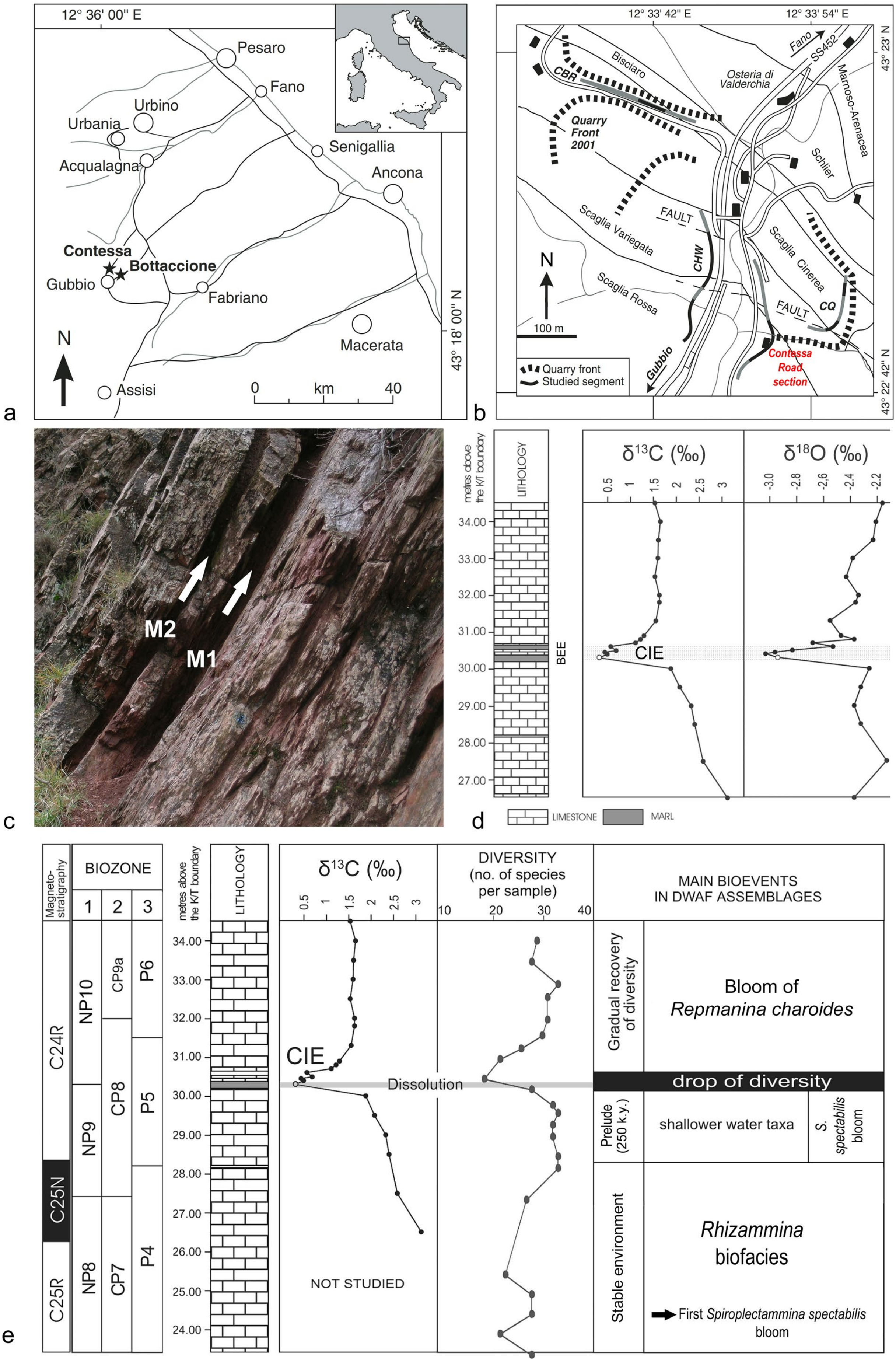
a
12° 36' 00'' E
43° 18' 00'' N
Pesaro
Fano
Urbino
Urbania
Senigallia
Acqualagna
Ancona
Contessa
Bottaccione
Gubbio
Fabriano
Macerata
Assisi
N
0
km
40
b
12° 33' 42'' E
12° 33' 54'' E
43° 23' N
43° 22' 42'' N
Fano
SS452
Bisciaro
CBR
Osteria di Valderchia
Marnoso-Arenacea
Quarry Front 2001
Schlier
FAULT
Scaglia Variegata
Scaglia Cinerea
CHW
N
Scaglia Rossa
FAULT
CQ
100 m
Contessa Road section
Quarry front
Studied segment
Gubbio
c
M2
M1
d
metres above the K/T boundary
LITHOLOGY
δ13C (‰)
δ18O (‰)
BEE
CIE
LIMESTONE
MARL
e
Magneto-stratigraphy
BIOZONE
1
2
3
C24R
C25N
C25R
NP10
NP9
NP8
CP9a
CP8
CP7
P6
P5
P4
metres above the K/T boundary
LITHOLOGY
δ13C (‰)
CIE
Dissolution
NOT STUDIED
DIVERSITY (no. of species per sample)
MAIN BIOEVENTS IN DWAF ASSEMBLAGES
Gradual recovery of diversity
Bloom of Repmanina charoides
drop of diversity
Prelude (250 k.y.)
shallower water taxa
S. spectabilis bloom
Stable environment
Rhizammina biofacies
First Spiroplectammina spectabilis bloom

Recently, integrated bio-magneto and chronostratigraphic studies on five Palaeogene key sections from the historical Contessa Valley and Bottaccione Gorge exposures (Fig. 1b), allowed reconstructing a complete composite succession, ~250 m-thick, covering the entire Palaeogene interval (PPCS; Coccioni et al., 2016). The component segments of the PPCS are internationally recognised as standards for the Palaeogene geomagnetic polarity time scale (GPTS), calibrated to the integrated calcareous plankton and dinocysts biostratigraphy, which provided reference for the geologic time scale of Gradstein et al. (2012). The lower Palaeogene succession of Gubbio was object of pioneering stratigraphic investigations since the 1930s (e.g., Renz, 1936; Luterbacher, 1964; Luterbacher & Premoli Silva, 1964; Monechi & Pirini Raddrizzani, 1975; Alvarez et al., 1977; Lowrie et al., 1982; Napoleone et al., 1983; Monechi & Thierstein, 1985, among others) and became of worldwide importance after Alvarez et al. (1980) proposed the bolide impact hypothesis as the cause for the K/Pg mass extinction. After the early studies on the PETM at the Contessa Road section (see below), the researches on the Umbria-Marche Palaeogene record moved to the less documented early Palaeogene climatic events, such as the Dan-C2, the ELPE, the Eocene Thermal Maximum 3 and the Middle Eocene Climatic Optimum (e.g., Jovane et al., 2007; Coccioni et al., 2010; Frontalini et al., 2016; Coccioni et al., 2019).

The Contessa Road section

At about the same time of the publication of the fundamental paper of Kennett & Stott (1991) on the discovery of the "end Palaeocene event" in ODP sediments (Hole 690, Weddell Sea, Antarctica), Corfield et al. (1991) published the first Cretaceous to Palaeogene stable isotope record with reliable time control from a spliced on-land section, including the Bottaccione Gorge and Contessa Highway records. This isotope record included an uncommented negative $\delta^{13}C$ shift at the Palaeocene-Eocene transition, which was however poorly documented because of tectonic and sedimentary disturbances that occurred in both the component sections at that stratigraphic level.

Later, Galeotti et al. (2000) investigated and acknowledged the Contessa Road section, belonging the Scaglia Rossa and Scaglia Variegata formations (Fig. 1b), as suitable for the study of the P/E transition. The section, previously studied by Luterbacher (1964) and Lowrie et al. (1982), belongs to Member R3 of the Scaglia Rossa Formation of Alvarez & Montanari (1988) and provides the only (virtually) complete record of the PETM available in the area. The local lithology is dominated by reddish limestones and marly limestones, with bedding ranging in thickness from ~ 0.5 cm to ~10 cm. After an integrated bio-magnetostratigraphic and isotopic study of a 10 m-thick interval, Galeotti et al. (2000) documented the presence of two distinctive marly layers in the interval between 30.30 m and 30.70 m above the K/Pg boundary (Fig. 1c-d). The lower layer, ~10 cm-thick, was interpreted as the Carbonate Dissolution Interval (CDI) reported in several PETM on-land sections and ODP sites. At its base, both the onset of a 40 cm-thick carbon isotopes excursion (CIE; Fig. 1d) and the benthic foraminiferal extinction event (BEE) were detected. The study of Galeotti et al. (2000) represented the first opportunity to compare and mutually calibrate the records from calcareous plankton, magnetostratigraphy and stable isotopes across the PETM interval in Italy, and allowed investigating the faunal turnover of calcareous and agglutinated benthic foraminifera. Galeotti et al. (2000) also observed that a gradual change in agglutinated foraminiferal assemblages begun well before the BEE, as testified by the entrance of outer neritic-bathyal agglutinated foraminifera at lower bathyal settings. Galeotti et al. (2004; Fig. 1e) collected further information on this event from the same section, pointing to a general re-organisation of the deep-water masses during the last 750 k.y. of the late Palaeocene, which probably intensified about 250 k.y. prior to the BEE, as also testified by two separate blooms of the opportunistic agglutinated species *Spiroplectammina spectabilis* (Grzybowski, 1898). Such changes were interpreted as the response to significant re-organisation of intermediate and deep-water masses following the onset of deep convection in the western Tethys. Above the CIE, a bloom of ammodiscids as *Repmanina charoides* (Jones & Parker, 1860), widely documented in many Tethys and Atlantic sites during the lowermost Eocene, was also observed (Fig. 1e). This bloom, initially explained as the response to extensive shallowing of the CCD, was recently interpreted as a consequence of massive inputs of refractory organic matter, possibly associated with pulses of terrigenous and/or siliciclastic material to deep-sea floor (e.g., Arreguín-Rodríguez et al., 2014).

The Contessa Road section was also part of a comprehensive study (Angori et al., 2007; Fig. 2a) aimed at documenting the response of calcareous nannoplankton communities to the PETM event in selected Tethyan sections, compared to the high-latitude reference record of ODP Site 690 (Weddell Sea). Sharp increases of r-selected taxa (e.g., the genera *Biscutum* Black in Black & Barnes, 1959 and *Prinsius* Hay & Mohler, 1967) pre-dating the PETM were observed in both sectors, which possibly reflect the onset of eutrophic conditions in surface waters in response to episodic upwelling pulses (Angori et al., 2007). These evidences suggest that the ocean system was perturbed well before the onset of the CIE (Fig. 2a). The Tethyan calcareous nannoplankton record shows that a dramatic drop occurred in calcareous nannoplankton diversity and abundance in coincidence with the BEE and paralleled by the appearance of a *Rhomboaster* Bramlette & Sullivan, 1961-*Discoaster araneus* Bukry, 1971 assemblage (R-D assemblage of Kahn & Aubry, 2004 or the CNET, "calcareous nannofossil excursion taxa"; see Agnini et al., 2006 and references therein). The latter assemblage characterises the CIE interval, pointing to stressed conditions at the ocean surface. The recovery to "standard" conditions in the calcareous nannofossils community was achieved later in the Tethys than at high latitudes in the Southern Hemisphere, where it occurred even prior to the CIE recovery. In both high latitudes and Tethys, however, the post-CIE assemblages indicate the persistence of stressed conditions (Angori et al., 2007).

Giusberti et al. (2009) provided a detailed analysis of the calcareous benthic foraminiferal response to the PETM in the Contessa Road section (Fig. 2b-c). Based on the overall faunal content, the palaeobathymetry of the site was assessed at depths not exceeding 1000-1500 m, slightly shallower than previous estimates (e.g., Galeotti et al., 2004). This study also revealed the consistent presence of buliminids as *Siphogenerinoides brevispinosa* Cushman, 1939 and *Rectobulimina carpentierae* Marie, 1956, previously documented at the PETM only in ODP Sites (e.g., Thomas & Shackleton, 1996; Thomas, 2003, 2007; Fig. 2b). A significant change in the taxonomical structure of benthic foraminiferal assemblages was recognised ~45 k.y. before the BEE suggesting unstable conditions at the seafloor as precursors of the PETM, as later observed in other sites (e.g., Giusberti et al., 2016; Alegret et al., 2018). The BEE was pinned precisely in the mid portion of the lower marly bed ("M1"), previously described and interpreted by Galeotti et al. (2000, 2004) as equivalent to the CDI (Fig. 2c). A second interval of dissolution, however less severe than the previous, was recognised in the middle part of the upper marly unit "M2" (uppermost part of the main CIE interval). This interval, interpreted as a repeated yet less pronounced shoaling of the lysocline/CCD that hampered the recovery of benthic faunas (Fig. 2b-c), suggests that the ocean geochemistry was persistently unstable in this sector of the Tethys before the CIE ended (Giusberti et al., 2009). Intervals of decreased calcite content or dissolution have been observed at a similar stratigraphic position in other Tethyan PETM records (e.g., Ortiz, 1995; Luciani et al., 2007; Alegret et al., 2009), but further investigations are required. Based on geochemical and microfaunal evidences, Giusberti et al. (2009) concluded that the lower part of the CIE in the Contessa section is represented by a complete yet extremely condensed record. Galeotti et al. (2010) studied a more expanded profile of the Contessa Road section, from 26 to 53 m above the K/Pg boundary, including the PETM and the overlying Ypresian hyperthermals ETM2 and ETM3, by means of an integrated bio-magneto-cyclostratigraphic approach. The authors concluded that the two post-PETM hyperthermals took place under conditions of maximal insolation within a very long period of eccentricity modulation (ca. 1.2 M.y.), thus suggesting that the orbital control on insolation might have played a key role in triggering both the ETM2 and ETM3 events. Also based on the astronomically-calibrated cyclostratigraphic record of the Contessa Road, De Conto et al. (2012) concluded that the magnitude and timing of the PETM, as well as the following hyperthermals, can be explained by the decay of organic carbon stored in soils of circum-Arctic and Antarctic terrestrial permafrost in response to orbital forcing (the so-called "permafrost" theory).

More recently, the PETM record from the Umbria-Marche region was included in a high-resolution geochemical stratigraphy reconstructed in the composite Contessa Road-Bottaccione section (CRBTT), which allowed to test the global significance of early Eocene short- and long-term carbon isotope trends by comparison with ocean records worldwide (Galeotti et al., 2017). The recognition of orbitally-forced sedimentary cycles at the CRBTT, interpreted as the response to long- (405 k.y.) and short- (100 k.y.) eccentricity periods, permitted a straightforward correlation to the Walvis Ridge ODP Sites records (southern Atlantic Ocean). Accordingly, the main hyperthermal events were framed within an unambiguous magnetostratigraphic record in the interval straddling the Early Eocene Climatic Optimum, which allowed for a refined astrochronological interpretation of the Ypresian Stage (Galeotti et al., 2017).

THE PETM RECORD IN THE SOUTHERN ALPS OF NORTHEASTERN ITALY

A "Scaglia"-type pelagic-hemipelagic succession, very similar to that exposed in the Umbria-Marche region, is also well preserved in the eastern Southern Alps (Veneto region, northeastern Italy; Fig. 3a). This succession is well known in the literature thanks to its contribution to the Cretaceous and Palaeogene stratigraphy (e.g., Bolli, 1975; Channell et al., 1979; Channell & Grandesso, 1987; Channell et al., 1987). These sedimentary successions were mainly deposited at middle to lower bathyal depths in the so-called Belluno Basin (BB), a Mesozoic-Palaeogene palaeogeographic unit of the European Southern Alps. The BB probably consisted in an embayment connected to the western Tethys at a palaeolatitude of ca. 42° during the early Eocene (Luciani et al., 2016). Traditionally, only the shallow-water, richly fossiliferous Palaeogene successions preserved in the central-western part of the Veneto region (e.g., Fabiani, 1915) were investigated thoroughly since the Reinassance (e.g., the fish-bearing Ypresian Fossil-Lagerstatte of Bolca; see Marramà et al., 2016). On the contrary, the deep-sea regional stratigraphy of the Palaeogene was scarcely documented (Poletti et al., 2004), as only the deep-sea succession exposed in the surroundings of the village of Possagno (Treviso province; Fig. 3a-b) was studied in depth during the 1970s (Bolli, 1975). The expanded lower Palaeogene succession of the northeastern part of the region remained for decades virtually unknown to the international scientific community, although the area was one of the first localities where the benthic foraminiferal extinction event associated with the Palaeocene-Eocene transition was recognised (Di Napoli Alliata et al., 1970). In the early 2000s, the "Palaeogene Veneto Project" (PVP), coordinated and promoted by Prof. D. Rio from the University of Padova

Fig. 2 (next page) - The Contessa Road PETM record. a) Calcareous nannofossil assemblages across the P-E transition: correlation between ODP Site 690 and Tethyan sections (based on data from Alamedilla, Caravaca, Zumaia [Spain], Contessa [central Italy], and Wadi Nukhl [Egypt] sections; Angori et al., 2007). The green band indicates the core of the negative carbon isotope excursion (CIE) interval. Redrawn from Angori et al. (2007). b) Relative abundance of selected benthic foraminifera across the Palaeocene/Eocene boundary at Contessa Road plotted against the recognised assemblages (A to H), the $\delta^{13}C$ and barite content records together with the isotopic intervals. "Extinction taxa" includes the species listed in Giusberti et al. (2009, Table 1). Benthic foraminiferal zonation after Berggren & Miller (1989). Modified after Giusberti et al. (2009). c) Main benthic foraminiferal events, assemblages, environmental conditions and isotopic intervals across the Palaeocene/Eocene boundary at Contessa Road. The stratigraphic intervals containing assemblages A-B, C and D-H are the pre-extinction, extinction and repopulation intervals, respectively. BL: Burndown Layer; CDI: Carbonate Dissolution Interval. Benthic foraminiferal zonation after Berggren & Miller (1989).

Fig. 2

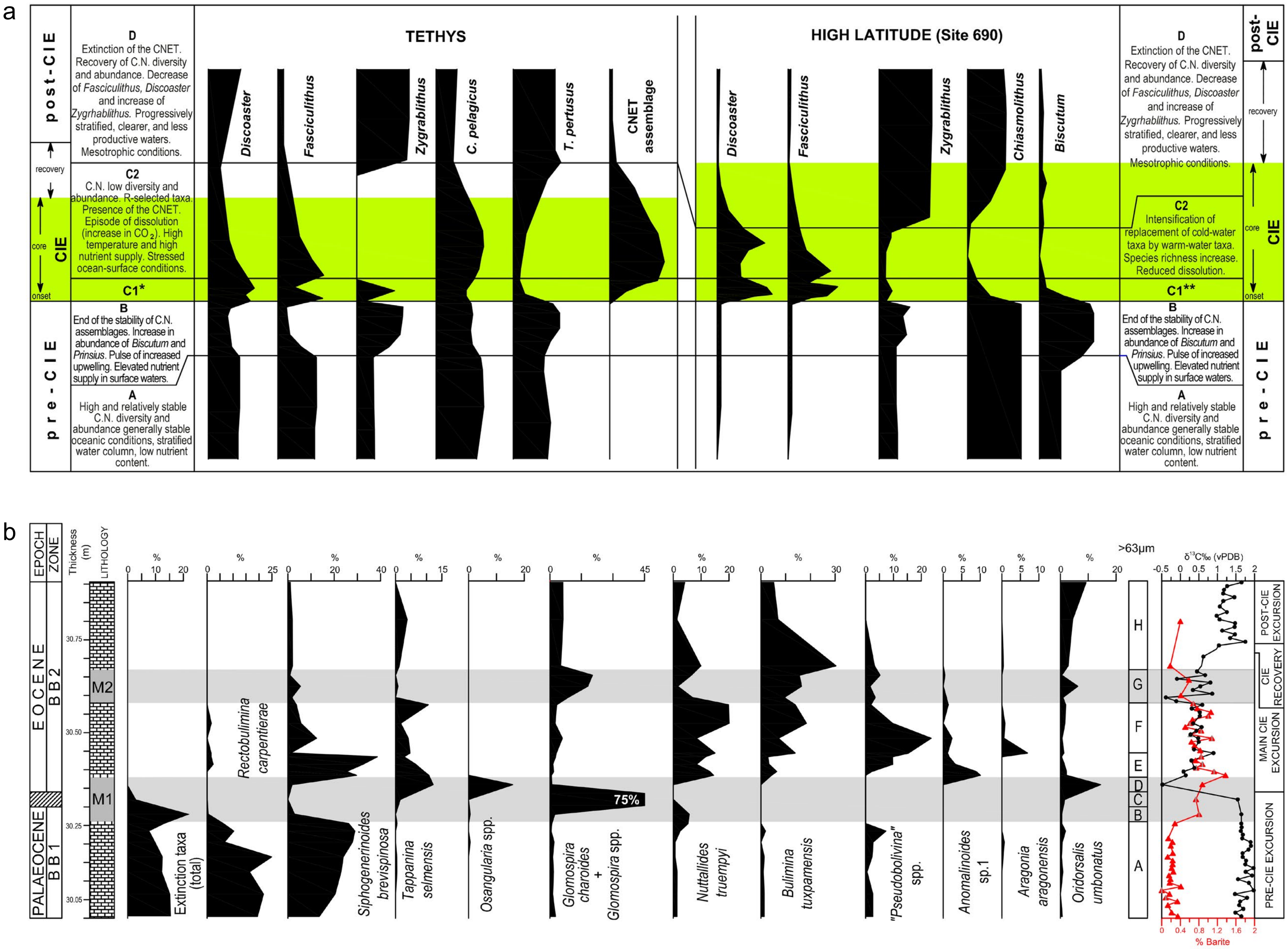
a
TETHYS
HIGH LATITUDE (Site 690)
post-CIE
pre-CIE
CIE
recovery
core
onset
D
Extinction of the CNET. Recovery of C.N. diversity and abundance. Decrease of Fasciculithus, Discoaster and increase of Zygrhablithus. Progressively stratified, clearer, and less productive waters. Mesotrophic conditions.
C2
C.N. low diversity and abundance. R-selected taxa. Presence of the CNET. Episode of dissolution (increase in CO2). High temperature and high nutrient supply. Stressed ocean-surface conditions.
C1*
B
End of the stability of C.N. assemblages. Increase in abundance of Biscutum and Prinsius. Pulse of increased upwelling. Elevated nutrient supply in surface waters.
A
High and relatively stable C.N. diversity and abundance generally stable oceanic conditions, stratified water column, low nutrient content.
Discoaster
Fasciculithus
Zygrablithus
C. pelagicus
T. pertusus
CNET assemblage
Discoaster
Fasciculithus
Zygrablithus
Chiasmolithus
Biscutum
C2
Intensification of replacement of cold-water taxa by warm-water taxa. Species richness increase. Reduced dissolution.
C1**
b
EPOCH
ZONE
Thickness (m)
LITHOLOGY
PALAEOCENE
EOCENE
BB1
BB2
M1
M2
30.05
30.25
30.50
30.75
%
75%
Extinction taxa (total)
Rectobulimina carpentierae
Siphogenerinoides brevispinosa
Tappanina selmensis
Osangularia spp.
Glomospira charoides + Glomospira spp.
Nuttallides truempyi
Bulimina tuxpamensis
"Pseudobolivina" spp.
Anomalinoides sp.1
Aragonia aragonensis
Oridorsalis umbonatus
>63µm
δ13C‰ (vPDB)
% Barite
A
B
C
D
E
F
G
H
PRE-CIE EXCURSION
MAIN CIE EXCURSION
CIE RECOVERY
POST-CIE EXCURSION

Fig. 2

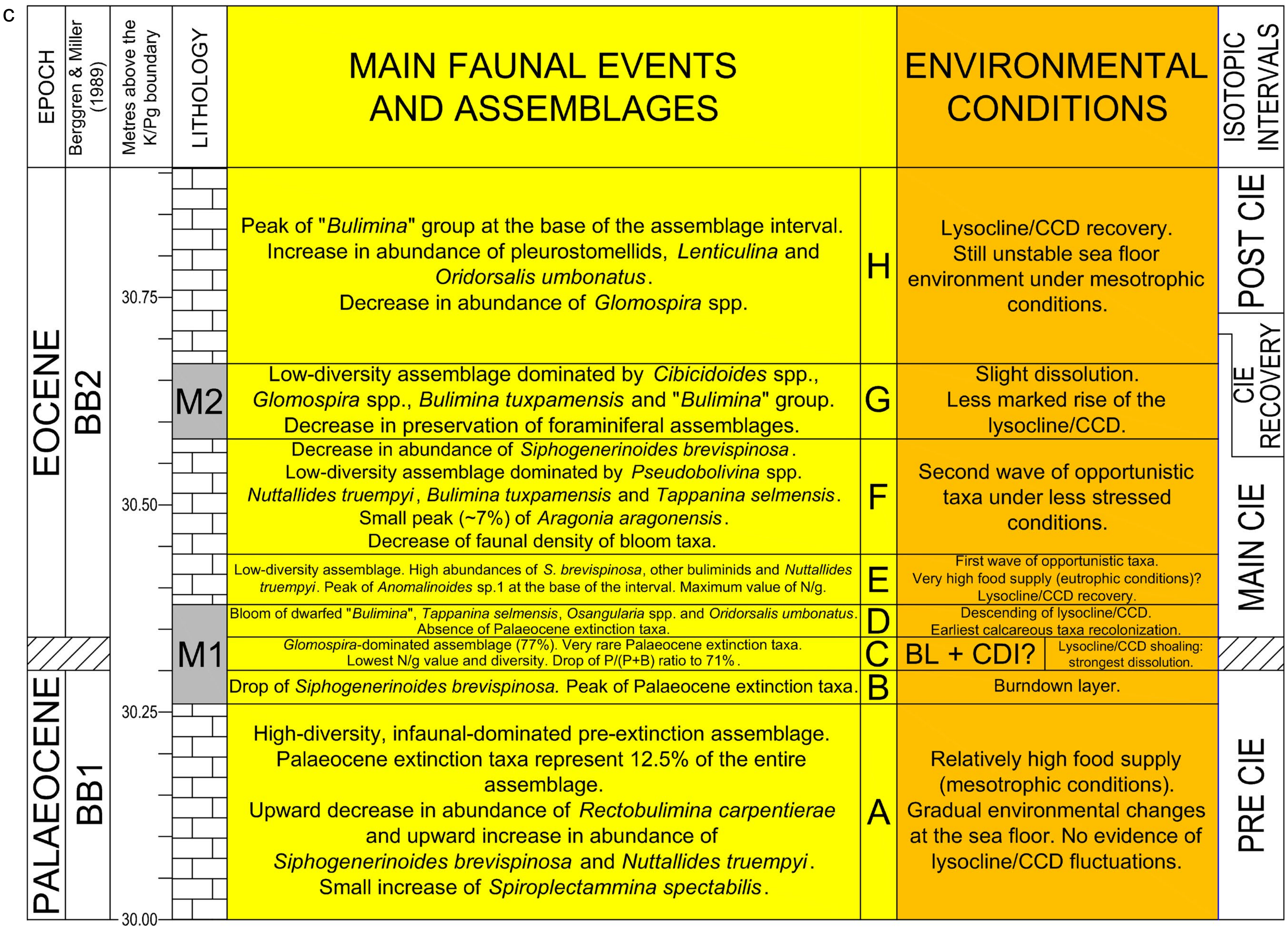
c
EPOCH
Berggren & Miller (1989)
Metres above the K/Pg boundary
LITHOLOGY
MAIN FAUNAL EVENTS AND ASSEMBLAGES
ENVIRONMENTAL CONDITIONS
ISOTOPIC INTERVALS
EOCENE
PALAEOCENE
BB2
BB1
30.75
30.50
30.25
30.00
M2
M1
Peak of "*Bulimina*" group at the base of the assemblage interval. Increase in abundance of pleurostomellids, *Lenticulina* and *Oridorsalis umbonatus*. Decrease in abundance of *Glomospira* spp.
H
Lysocline/CCD recovery. Still unstable sea floor environment under mesotrophic conditions.
Low-diversity assemblage dominated by *Cibicidoides* spp., *Glomospira* spp., *Bulimina tuxpamensis* and "*Bulimina*" group. Decrease in preservation of foraminiferal assemblages.
G
Slight dissolution. Less marked rise of the lysocline/CCD.
Decrease in abundance of *Siphogenerinoides brevispinosa*. Low-diversity assemblage dominated by *Pseudobolivina* spp. *Nuttallides truempyi*, *Bulimina tuxpamensis* and *Tappanina selmensis*. Small peak (~7%) of *Aragonia aragonensis*. Decrease of faunal density of bloom taxa.
F
Second wave of opportunistic taxa under less stressed conditions.
Low-diversity assemblage. High abundances of *S. brevispinosa*, other buliminids and *Nuttallides truempyi*. Peak of *Anomalinoides* sp.1 at the base of the interval. Maximum value of N/g.
E
First wave of opportunistic taxa. Very high food supply (eutrophic conditions)? Lysocline/CCD recovery.
Bloom of dwarfed "*Bulimina*", *Tappanina selmensis*, *Osangularia* spp. and *Oridorsalis umbonatus*. Absence of Palaeocene extinction taxa.
D
Descending of lysocline/CCD. Earliest calcareous taxa recolonization.
Glomospira-dominated assemblage (77%). Very rare Palaeocene extinction taxa. Lowest N/g value and diversity. Drop of P/(P+B) ratio to 71%.
C
BL + CDI?
Lysocline/CCD shoaling: strongest dissolution.
Drop of *Siphogenerinoides brevispinosa.* Peak of Palaeocene extinction taxa.
B
Burndown layer.
High-diversity, infaunal-dominated pre-extinction assemblage. Palaeocene extinction taxa represent 12.5% of the entire assemblage. Upward decrease in abundance of *Rectobulimina carpentierae* and upward increase in abundance of *Siphogenerinoides brevispinosa* and *Nuttallides truempyi*. Small increase of *Spiroplectammina spectabilis*.
A
Relatively high food supply (mesotrophic conditions). Gradual environmental changes at the sea floor. No evidence of lysocline/CCD fluctuations.
POST CIE
CIE RECOVERY
MAIN CIE
PRE CIE

renewed the interest in the deep-sea Palaeogene record of Veneto, and regional biostratigraphic studies - paralleled by interdisciplinary investigations on Palaeogene climate - got under way (Rio et al., 2003; Agnini et al., 2014a). The regional biostratigraphic knowledge collected during fourteen years of investigation was fundamental for establishing a new low- to mid-latitude Palaeogene calcareous nannofossil zonation (Agnini et al., 2014b) and for a critical reassessment of the Eocene planktic foraminiferal biostratigraphy (e.g., Luciani & Giusberti, 2014). Such results provided the tools for time telling on some poorly dated Palaeogene records of western Veneto region (Giusberti et al., 2014; Papazzoni et al., 2017) and were fundamental for proposing a GSSP candidate for the Priabonian Stage (Agnini et al., 2011). Early investigations performed in the framework of the PVP were initially focused on the iconic PETM, but eventually led to the discovery in the region of key records of climatic extreme events of the Palaeogene, such as the ETM2 (D'Onofrio et al., 2016), the ETM3 (Agnini et al., 2009) and the Middle Eocene Climatic Optimum (MECO; e.g., Boscolo Galazzo et al., 2013 and references therein).

The Possagno section (*Carcoselle Quarry, Treviso*)

Modern investigations on the PETM in northern Italy started at the end of the 1990s, when Arenillas et al. (1999) studied the planktic foraminiferal record of the Carcoselle Quarry section, in the outskirts of Possagno (Fig. 3b-d). The site was internationally known since the publication of the monograph by Bolli (1975), and was cited in the seminal paper of Kennett & Stott (1991) as one of the three on-land sections where the BEE was first documented (Braga et al., 1975). Here, Arenillas et al. (1999) recognised the PETM close to the transition between the Scaglia Rossa and "Scaglia Variegata" formations, in correspondence to a 1 m-thick interval of red marls and limestones that contain a 4 cm-thick dark red clay layer characterised by dissolution, seemingly coinciding with the BEE (Fig. 3c-d). The $\delta^{13}C$ record of the Carcoselle section revealed a 35-40 cm-thick, thus very condensed CIE. Within this interval, in agreement with any other section investigated so far in the Tethys and North Atlantic, planktic foraminiferal assemblages show a low-latitudes acarininid incursion, which allegedly occurred in response to the peak P/E warming (Arenillas et al., 1999; Molina et al., 1999; Fig. 3c). The onset of such warm-water taxa incursion, as recorded at Possagno and in other Spanish sections, preceded the onset of the CIE and was possibly associated to the massive spawning of warm-water masses prior to the PETM (Arenillas et al., 1999; Fig. 3c). The Palaeocene-Eocene transition at Possagno was framed within the planktic foraminiferal subzonation of Molina et al. (1999), one of the first attempts to refine the biozones P4-P6 of Berggren et al. (1995), valid for low and middle latitudes. Specifically, Molina et al. (1999) subdivided the 1.4 M.y.-long P5 Zone into 5 subzones, with the aim of constraining the "P/E boundary events" within a more resolved biostratigraphic framework. Based on this pioneer work, Berggren & Pearson (2005) adopted a twofold subdivision of the upper part of (former) Zone P5 in their revised planktic foraminiferal Palaeogene biozonation. In particular, the LO of the "excursion taxon" *Acarinina sibaiyaensis* (El Naggar, 1966) (one of the events highlighted by Molina et al., 1999) was selected as biohorizon for defining the first Eocene Zone (E1). Such subdivision was adopted later by Wade et al. (2011) in their revised Cenozoic tropical planktic foraminiferal zonation. At the beginning of the 2000s, the discovery of expanded records of the PETM in the nearby Valbelluna (see below) partly diverted the scientific attention from the Carcoselle Quarry section. The latter, however, was subjected to broad investigations aimed at exploring the bio-magnetostratigraphic record and documenting the transient modifications and true evolutionary trends in calcareous plankton through the upper Palaeocene-middle Eocene interval (e.g., Agnini et al., 2006; Luciani & Giusberti, 2014; Luciani et al., 2016).

The Valbelluna area and the discovery of the CMU

Along the southern flank of the Piave River Valley, known as the Valbelluna (Belluno province; Figs 3a, 4a), an Upper Cretaceous to lower Eocene sedimentary succession is widely exposed. It consists of locally rhythmically bedded pelagic to hemipelagic rocks, attaining to thicknesses of about 200-250 m (Fig. 4b; Giusberti et al., 2007). These rocks are traditionally referred to as "Scaglia Rossa" sensu lato, which includes lithostratigraphic units that still need formal ratification and/or revision (Dallanave et al., 2009). Field researches carried out in the early 2000s within the PVP context allowed for the recognition of four Palaeocene-lower Eocene sections suitable for integrated, high-resolution stratigraphic studies (Fig. 4c). These sections are characterised by marked differences in sedimentary facies and thicknesses, due to the dissimilar terrigenous content and the variable occurrence of redeposited shelf material in the Danian interval (Fig. 4c). Despite this lithological variability, an ubiquitous character of the lower Palaeogene stratigraphy in the Valbelluna is a 3 to 4 m-thick package of reddish and greenish marly clays and clayey marls known as the "clay marl unit" (CMU; Giusberti et al., 2007), which is interbedded within the background carbonate sediments (Fig. 4c-d). Such lithological anomaly marks regionally the PETM (Giusberti et al., 2007) and correlates well with analogous clay-rich units found globally on continental margins (e.g., the Siliciclastic Unit-SU of Schmitz et al., 2001). The base of the CMU corresponds to the Palaeocene/Eocene boundary as defined biostratigraphically (e.g., BEE), and the entire unit coincides with the main CIE associated with the PETM event, as demonstrated by the $\delta^{13}C$ record from bulk rock (Fig. 5a-b). In Valbelluna, the Palaeocene-Eocene transition interval is characterised by a pervasive lithologic cyclicity, that is documented immediately

Fig. 3 - The PETM record at Possagno. a) Location map of the northeastern Italy sites cited in the text: Possagno and Valbelluna area (rectangle). b) The exposed quarry face of Carcoselle (Possagno) exposing the upper Palaeocene-Lutetian interval (summer 2002). c) Biostratigraphy, relative abundance of planktonic foraminifera and $\delta^{13}C$ curve across the Palaeocene/Eocene boundary at Carcoselle quarry. BEE: benthic foraminiferal extinction event; CIE: Carbon isotope excursion. 1: calcareous marls; 2: marls and clays (CMU: clay marl unit); 3: limestones. Redrawn from Molina et al. (1999). d) The Palaeocene-Eocene transition at Carcoselle Quarry. CMU: clay marl unit.

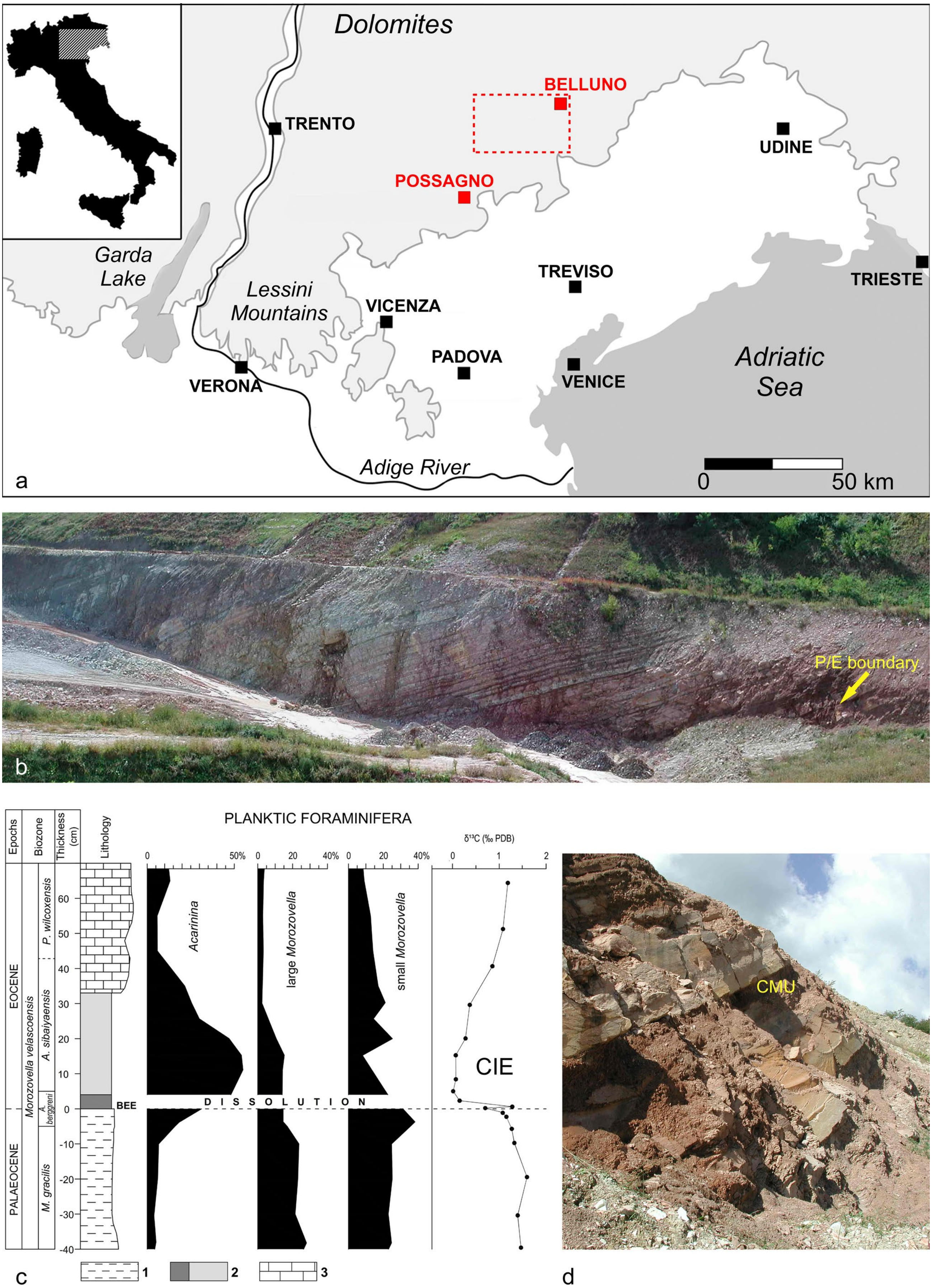
Dolomites
BELLUNO
TRENTO
UDINE
POSSAGNO
Garda
Lake
Lessini
Mountains
TREVISO
TRIESTE
VICENZA
PADOVA
VERONA
VENICE
Adriatic
Sea
Adige River
0
50 km
a
P/E boundary
b
PLANKTIC FORAMINIFERA
Epochs
Biozone
Thickness (cm)
Lithology
EOCENE
PALAEOCENE
Morozovella velascoensis
P. wilcoxensis
A. sibaiyaensis
A. berggreni
M. gracilis
BEE
Acarinina
large Morozovella
small Morozovella
DISSOLUTION
δ13C (‰ PDB)
CIE
0
50%
20
40%
1
2
1
2
3
c
CMU
d

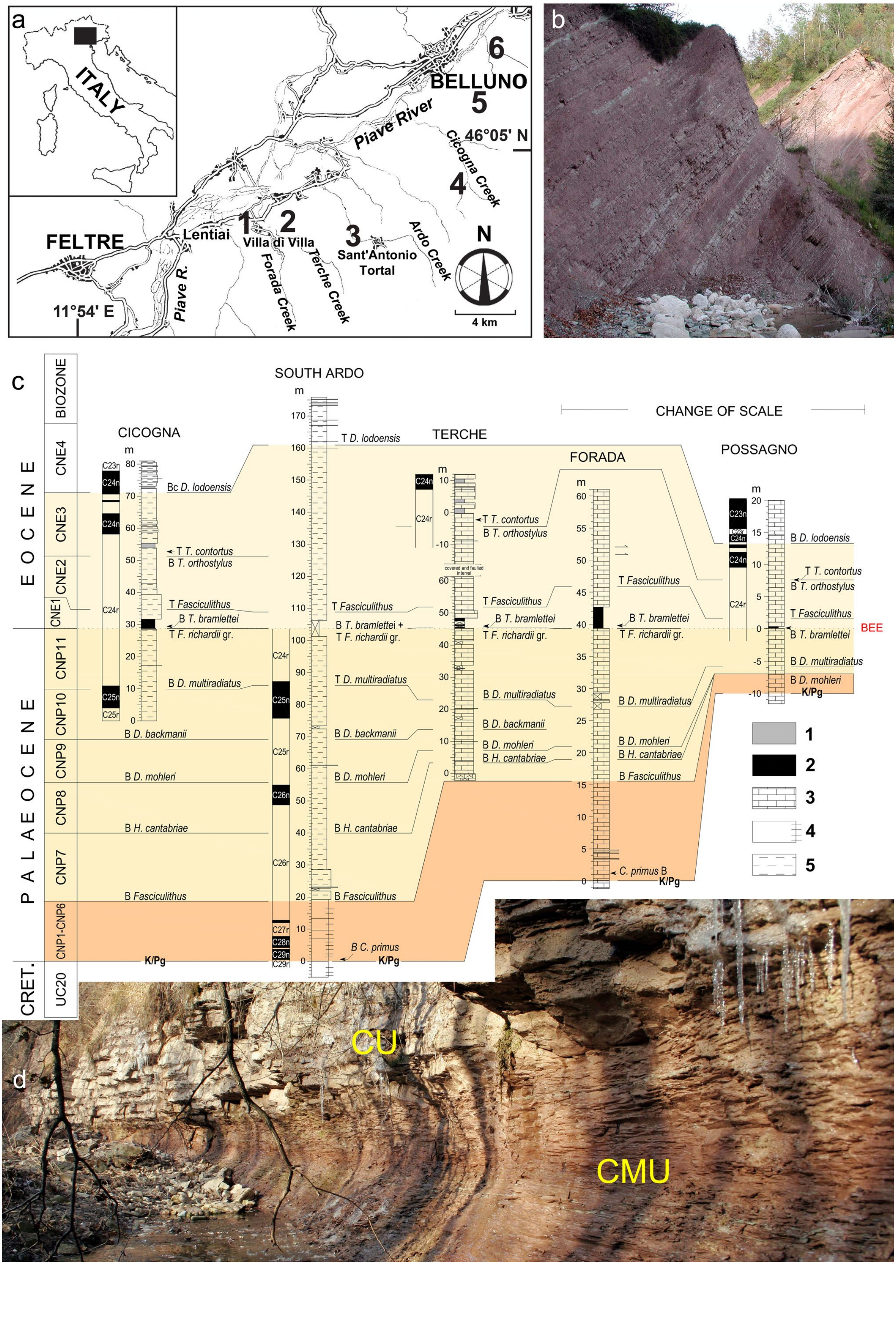
a
ITALY
FELTRE
Lentiai
1
2
Villa di Villa
3
Sant'Antonio
Tortal
4
5
6
BELLUNO
Piave River
Piave R.
Forada Creek
Terche Creek
Ardo Creek
Cicogna Creek
46°05' N
11°54' E
N
4 km
b
c
BIOZONE
E O C E N E
P A L A E O C E N E
CRET.
CNE4
CNE3
CNE2
CNE1
CNP11
CNP10
CNP9
CNP8
CNP7
CNP1-CNP6
UC20
CICOGNA
SOUTH ARDO
TERCHE
FORADA
POSSAGNO
CHANGE OF SCALE
m
Bc D. lodoensis
T T. contortus
B T. orthostylus
T Fasciculithus
B T. bramlettei
T F. richardii gr.
B D. multiradiatus
B D. backmanii
B D. mohleri
B H. cantabriae
B Fasciculithus
B C. primus
K/Pg
T D. lodoensis
B T. bramlettei +
T F. richardii gr.
T D. multiradiatus
covered and faulted interval
C. primus B
B D. lodoensis
BEE
C23r
C24n
C24r
C25n
C25r
C26n
C26r
C27r
C28n
C29n
C29r
C23n
1
2
3
4
5
CU
CMU
d

below and above the CMU, consisting of couplets of reddish marls and indurated marly limestones (Fig. 4d). The boundary between the CMU and the overlying marl-limestone couplets, known as the "couplet unit" (CU; Fig. 4d), is sharp (Giusberti et al., 2007; Dallanave et al., 2009). Among the numerous sites recording the PETM in the Valbelluna area, the best section is exposed along the Forada Creek, where the CMU is easily accessible, well exposed and unaffected by tectonic disturbances (Figs 4a, c-d, 5a).

The PETM in the Forada section

The Forada section consists of ~62 m of reddish limestones and marls belonging to the Scaglia Rossa Formation, encompassing the uppermost Maastrichtian to lower Ypresian interval (Fornaciari et al., 2007; Fig. 5a). Component sediments were deposited in the central-eastern portion of the Belluno Basin, probably at depths between 1000 and 1500 m (Giusberti et al., 2016). The Palaeocene interval is represented by ~40 metres of reddish marls and marly limestones. Sediment accumulation rates are highly variable, because - against an expanded stratigraphic record of the lowermost Danian and the Thanetian - the Danian-Selandian interval is remarkably condensed (Fig. 5a). The CMU is ~3 m thick and is overlain by a 4-5 m thick CU that, in turn, fades into a 15 m-thick interval of scaly, yet still strongly cyclically-organised reddish marls (Figs 4d, 5a). The expanded PETM record preserved in the Forada section has been extensively studied over the years thanks to its continuity, microfossils abundance and cyclostratigraphy, thus becoming a firm reference for the Tethyan region (e.g., Agnini et al., 2007; Giusberti et al., 2007; Luciani et al., 2007; Tipple et al., 2011; Giusberti et al., 2016, 2018).

Cyclostratigraphy of the PETM - The entire CIE at Forada is ~4.8 m thick. It develops within an interval that is characterised not only by changes in carbonate content, carbon and oxygen isotopes, but also by significant changes in lithology, micropalaeontology, mineralogy, and chemistry (Fig. 5a-b). Such variability allowed for a subdivision of the CIE into six microstratigraphic intervals, beginning from shortly below the base of the CMU (Fig. 5b). Concentrations of hematite, $CaCO_3$, $\delta^{13}C$ values, as well as the abundance of radiolarians, oscillate cyclically according to frequencies that are interpreted as consistent with orbital precession cycles (Fig. 5b; Giusberti et al., 2007). The recognition of 11 precession-related cycles within the CIE interval implied that the PETM lasted between ca. 209 and 253 k.y., with an average of about 230 k.y. (Figs 5b, 6a) (Giusberti et al., 2007). The derived age model was the first attempt to obtain a cyclostratigraphically-derived chronology for the PETM in a marine on-land section. Röhl et al. (2007), in their attempt to compare the Forada record with the one of the ODP Site 690, objected that only eight cycles could be recognised within the CIE; accordingly, their estimated PETM duration was in the order of about 170 k.y., in stark contradiction with the conclusions of Giusberti et al. (2007) (Fig. 6). However, the ^{3}He-based chronology proposed later by Murphy et al. (2010) for ODP Site 1266 at Walvis Ridge indicated that the PETM lasted ~234 +48/-34 k.y., in good agreement with the previous age model proposed by Giusberti et al. (2007).

Huge terrestrial input at the PETM - The chronological framework developed by Giusberti et al. (2007) suggests that the sediment accumulation rates at Forada underwent a 3- to 5-fold increase in the interval straddling the PETM, being in the order of 7-10 m/M.y. in the upper Palaeocene and of about 33 m/M.y. for the basal Eocene, represented by the CMU/CIE main excursion. It must be stressed, however, that the estimates for the upper Palaeocene interval can vary significantly based on the employed age models. The sharp increase in sediment accumulation rates at Forada is consistent with what observed in continental sites (e.g., Charmichael et al., 2017 and references therein), where a dramatic change in the hydrological regime is documented during the super-greenhouse PETM that dramatically enhanced weathering and, consequently, the sediment yield to the basin margins. Giusberti et al. (2007) concluded that the hypothesis of increasing terrestrial inputs during the PETM was consistent with a scenario of extreme global warming and enhanced hydrological cycle, which might have triggered a pervasive silicate weathering via the permanent removal of excess atmospheric carbon. Recent studies in the Basque Zumaia section, which exhibits remarkable similarities with the Forada section, indicate nonetheless that silicate weathering alone was probably insufficient to recover from the PETM CIE, and the occurrence of active organic carbon burial processes was required in order to match the dynamics that are observed across the CIE (Dunkley Jones et al., 2018).

The calcareous nannofossil PETM record - Agnini et al. (2007) detailed the changes in calcareous nannoplankton assemblages across the PETM at Forada within the chronological, geochemical and mineralogical framework of Giusberti et al. (2007; Fig. 7). A sharp evidence is provided that the changes observed in the terrigenous input and mineralogical proxies at Forada

Fig. 4 - The most significant lower Palaeogene Valbelluna sections and the "clay marl unit". a) The Piave River Valley in the Belluno Province (the "Valbelluna") showing the location of the sections containing the Palaeocene-Eocene transition. 1: Forada Creek; 2: Terche Creek; 3: Ardo South Creek; 4: Cicogna Creek; 5: Madeago Valley; 6: Vena d'Oro Valley. b) Ypresian hemipelagic sediments of Scaglia Rossa Formation cropping out along the Cicogna Creek in Valbelluna (northeastern Italy), showing a prominent cyclicity. c) The simplified stratigraphy of the Cicogna, South Ardo, Terche and Forada sections (Giusberti et al., 2007; Dallanave et al., 2009, 2012a; D'Onofrio et al., 2016) and their correlation with the classical section of Possagno (Veneto region, NE Italy; Agnini et al., 2006) based on calcareous nannofossil biostratigraphy. From the bottom to the top, the coloured bands approximate the extension of the Danian (NP1-NP4), the Selandian-Thanetian (NP5-NP9a) and part of the Ypresian (NP9b-NP11) in the considered sections. 1: "marly unit" (MU: post-PETM hyperthermals); 2: clay marl unit (CMU); 3: Scaglia Rossa Formation; 4: "Cugnan formation"; 5: "Scaglia Cinerea formation" and "Marna della Vena d'Oro formation". d) Forada section: view of the upper part of the "clay marl unit" (CMU) and well-developed lower Eocene limestone-marl couplets ("couplets unit", CU). The base of CMU corresponds to the onset of the CIE. The interval of low $\delta^{13}C$ values has been recognised within the lithological anomaly, while the marl-limestone couplets represent the $\delta^{13}C$ recovery interval.

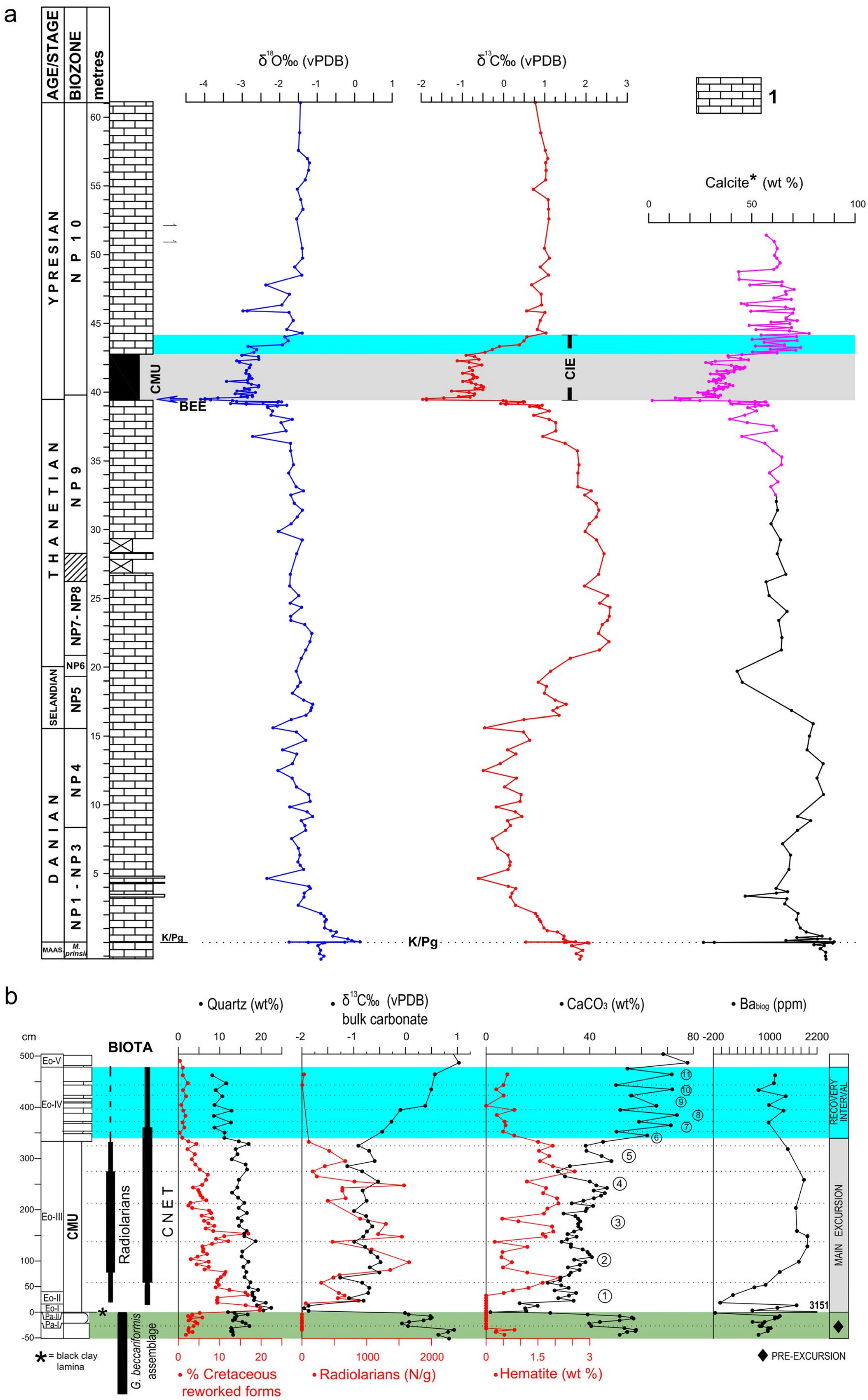
a
AGE/STAGE
BIOZONE
metres
δ18O‰ (vPDB)
δ13C‰ (vPDB)
1
Calcite* (wt %)
YPRESIAN
NP10
THANETIAN
NP9
NP7- NP8
NP6
SELANDIAN
NP5
DANIAN
NP4
NP1 - NP3
MAAS.
M. prinsii
CMU
BEE
CIE
K/Pg
b
cm
BIOTA
Eo-V
Eo-IV
Eo-III
Eo-II
Eo-I
Pa-II
Pa-I
CMU
Radiolarians
CNET
G. beccariformis assemblage
* = black clay lamina
• Quartz (wt%)
• δ13C‰ (vPDB) bulk carbonate
• CaCO3 (wt%)
• Babiog (ppm)
• % Cretaceous reworked forms
• Radiolarians (N/g)
• Hematite (wt %)
3151
RECOVERY INTERVAL
MAIN EXCURSION
PRE-EXCURSION

are in keeping with variations in nutrient supply, as demonstrated by a compelling correlation with changes in nannofossil assemblages. Accordingly, it is suggested that the fluctuations in surface waters conditions and the calcareous nannoplankton associations were linked by a persistent dynamic equilibrium (Agnini et al., 2007). Within the main CIE interval, oligotrophic taxa - such as *Sphenolithus* Deflandre, 1952, *Zygrhablithus* Deflandre, 1959, *Octolithus* Romein, 1979 and *Fasciculithus* Bramlette & Sullivan, 1961 - exhibit a sharp decrease in abundance. This trend is paralleled by both an increase in more eutrophic taxa (such as *Ericsonia* Black, 1964) and a peak of reworked Cretaceous taxa that, notably, has also been observed in the context of other hyperthermal records regionally. This event has been interpreted in terms of increased terrigenous discharge to the ocean in response to an enhanced hydrological cycle that, conceivably, also conveyed huge amounts of nutrients washed off from the mainland (e.g., Agnini et al., 2009; D'Onofrio et al., 2016). In support of this scenario is the evidence that the late- and post-CIE intervals show the return to more oligotrophic conditions, fully similar to those of the pre-CIE. The PETM at Forada also records both the emergence and extinction of ephemeral CNET taxa (*Discoaster anartios* Bybell & Self-Trail, 1995, *D. araneus* Bukry, 1971 and *Rhomboaster* spp.; Fig. 7), which have been interpreted as ecophenotypic malformations evolved in response to the changes in chemistry (nutrients, CO_2, pH) and temperature of the surface waters during the CIE (e.g., Agnini et al., 2007; Raffi & De Bernardi, 2008). Based on the age model developed for the P/E transition at Forada, Agnini et al. (2007) obtained a chronology for seven calcareous nannofossil biohorizons considered as reliable over wide areas in an interval of ca. 350 k.y. Among these, two were later adopted for the revised Palaeogene biozonation of Agnini et al. (2014b).

The planktic foraminiferal PETM record - Luciani et al. (2007) detected prominent changes in the abundance and composition of planktic foraminiferal assemblages at Forada (Fig. 8) that outlined a complex palaeoenvironmental evolution in the central-western Tethys across the PETM. About 150 k.y. before the onset of the CIE, an increase in subbotinids paralleled by a decrease in morozovellid suggests a marked environmental instability, involving a change from oligotrophy to eutrophy in the upper-column waters. Two prominent peaks in the abundance of acarininids were observed ca. 30 k.y. prior to the onset of the CIE, suggesting an increase in temperature heralding the onset of the PETM. Such increase, previously documented by Molina et al. (1999) in other Tethyan sites, commenced immediately below a -1‰ shift in $\delta^{13}C$, further supporting the hypothesis of a "PETM-prelude". The basal CIE at Forada is represented by a planktic foraminiferal dissolution interval (PFDI) lasting ca. 16 k.y. (Fig. 8). The utter dominance by acarininids in the lower part of the CIE (ca. 36 k.y.), coupled with the entry of abundant radiolarians, was interpreted as a consequence of extreme warming coupled with the onset of eutrophic conditions. The acarininid peak (Fig. 8) includes *Acarinina sibaiyaensis* (El Naggar, 1966) and *A. africana* (El Naggar, 1966), morphologically similar to the radially-elongated chambered forms that are documented to flourish during the Cretaceous anoxic events. Accordingly, Luciani et al. (2017) speculated that the oxygen depletion in the upper water column might have promoted the conspicuous occurrence of these "excursion taxa" during the PETM. Forms as *Acarinina sibaiyaensis* possibly thrived in nutrient-rich conditions as well (e.g., Ernst et al., 2006), which are demonstrated to occur within the CMU interval at Forada. In the upper part of the CIE at Forada (ca. 50 k.y.) planktic foraminifera indicate less stressed conditions that further improved in the overlying late CIE and post-CIE intervals (ca. 600 k.y.), where a diversified assemblage suggests a relatively stable and oligo-mesotrophic environment. Luciani et al. (2007) observed several first occurrences of new species within the "PETM prelude" and PETM intervals at Forada, which prompted the hypothesis that short-lived, yet severe, changes in the environmental conditions stimulated the speciation of planktic foraminifera, contrary to previous assumptions that related micro-evolutionary patterns in planktic foraminifera to both stable ocean conditions and depth-related specialisations.

Discarding a normal magnetic polarity event during the PETM - Lee & Odama (2009) reported the discovery of a normal polarity event (PEMR, Palaeocene-Eocene magnetic reversal, 39-53 k.y.-long; Dallanave et al., 2012b) within the 2.55 Myr-long Chron C24r at ODP Site 1262 (Walvis Ridge, South Atlantic Ocean), embedded within the clay layer interval of PETM. The authors speculated that the PEMR was possibly a global event related to a change in the Earth's rotation rate, influenced by an abrupt ocean-atmosphere circulation overturning that occurred during the PETM. Dallanave et al. (2012b) investigated in detail the expanded PETM record of Valbelluna in order to resolve the controversy regarding the existence of such a problematic event. The high-resolution palaeomagnetic and rock-magnetic dataset obtained from the Forada and nearby Cicogna sites (resolved temporally down to an average of ca. 3.3 k.y.) indicated that the entire CMU interval was deposited during a continuous interval of reverse geomagnetic field polarity, ruling out the occurrence of a magnetic polarity reversal throughout the PETM. Moreover, based

Fig. 5 - The Forada section stratigraphy. a) Simplified columnar log, calcareous nannofossil biostratigraphy, stable isotopes stratigraphy ($\delta^{13}C$ and $\delta^{18}O$ measured on bulk sample) and $CaCO_3$ of the entire upper Maastrichtian-Ypresian Forada section. Coloured bands denote the interval enclosing the basal Eocene carbon isotope excursion (main CIE and CIE recovery intervals). Calcite in the interval –122/+3205 cm was determined by recalculating chemical data (CaO and loss on ignition), whereas calcite in the interval +3252/+5142 cm was determined by coulometry. VPDB: Vienna Peedee belemnite standard; BEE: benthic foraminiferal extinction event; CMU: "clay marl unit"; K/Pg: Cretaceous/Palaeogene boundary; 1: Scaglia Rossa Formation. Modified after Giusberti et al. (2007). b) Summary of the main biotic, mineralogical, and cyclostratigraphic features recognised across the Palaeocene-Eocene boundary and in the CMU of the Forada section. Pa-I to Pa-II and Eo-I to Eo-IV denote the stratigraphic intervals recognised by Giusberti et al. (2007). Analyses of radiolarians and foraminifera are based on the fraction > 125 µm. CNET: calcareous nannofossil excursion taxa; VPDB: Vienna Peedee belemnite standard. Modified from Giusberti et al. (2007).

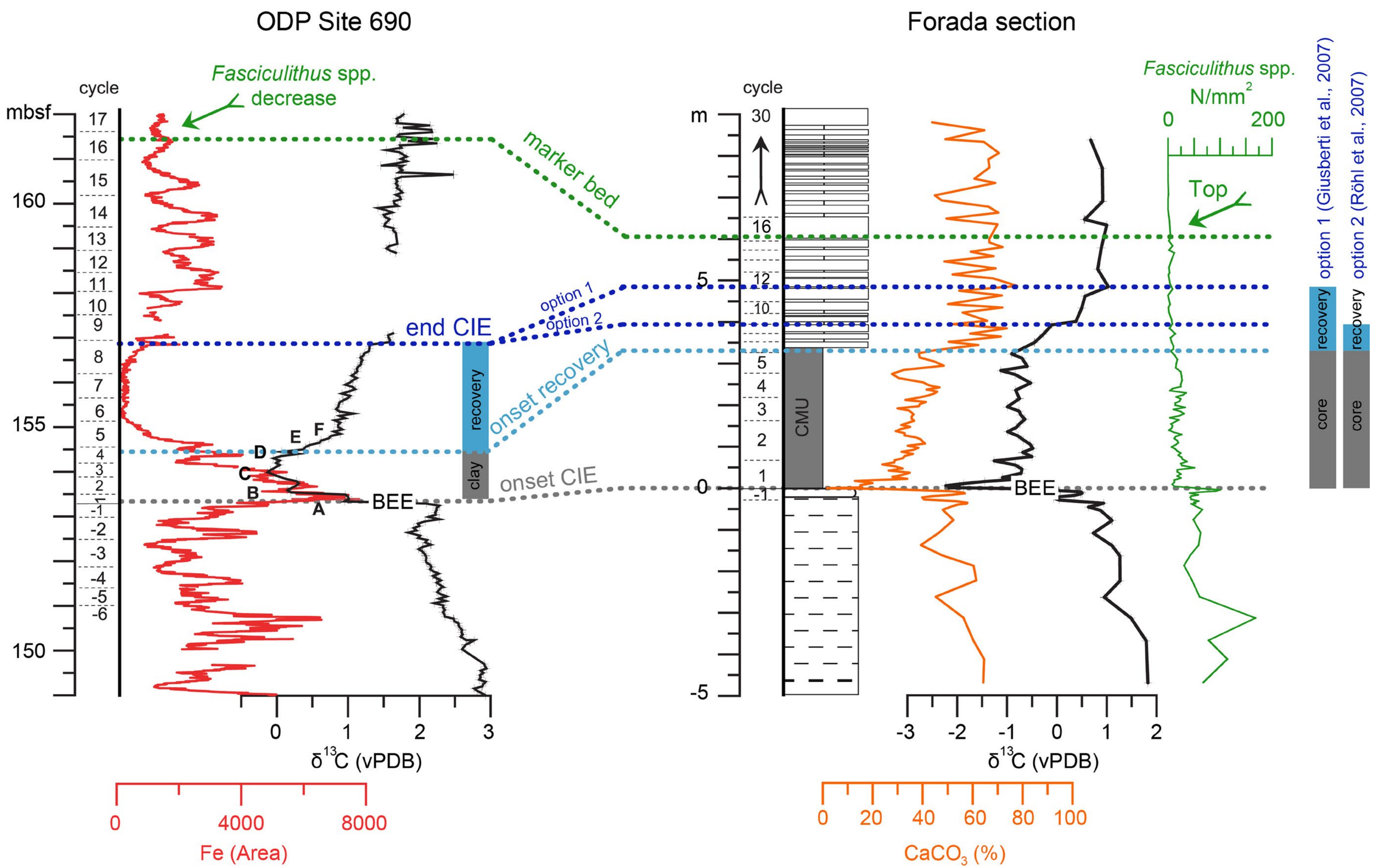

Fig. 6 - Cyclostratigraphy of the PETM at Forada section. Cyclostratigraphic correlation between ODP Site 690 (Weddel Sea) and the Forada section. ODP Site 690 Fe (total counts) and $\delta^{13}C$ data are after Röhl et al. (2007). $CaCO_3$ and $\delta^{13}C$ data are after Giusberti et al. (2007). Abundance pattern of calcareous nannofossil *Fasciculithus* spp. from Agnini et al. (2007). Letters (A-F) indicate horizons as identified by Zachos et al. (2005) for ODP Site 690. BEE: benthic foraminiferal extinction event. The blue dashed lines mark the position of the end of CIE according to Giusberti et al. (2007; Option 1) or Röhl et al. (2007; Option 2). For the lithology see Luciani et al. (2007, fig. 2), with the exception of the planktic foraminiferal dissolution interval (PFDI) at the base of CMU, here not reported. After Agnini et al. (2014a).

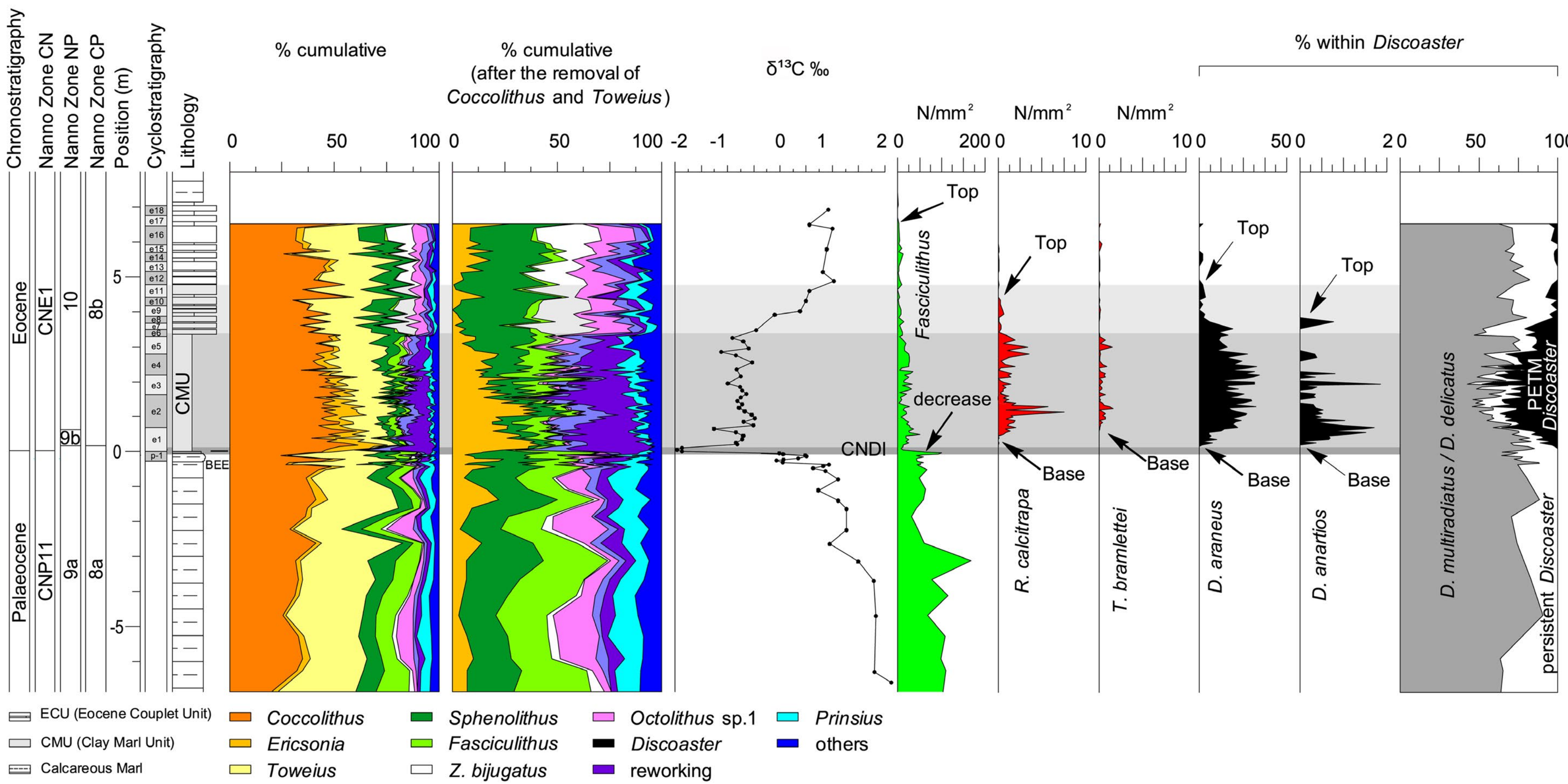

Fig. 7 - Calcareous nannofossil record in the interval straddling the PETM at Forada section. On the left, cumulative percentages before and after the removal of the *Coccolithus* Schwarz, 1894-*Toweius* Hay & Mohler, 1967 fraction are plotted against lithostratigraphy, chronostratigraphy, calcareous nannofossil biostratigraphy (NP: Martini, 1971; CP: Okada & Bukry, 1980; CN: Agnini et al., 2014b), lithology, cyclostratigraphy, and carbon isotopes. On the right, abundance patterns of selected calcareous nannofossil taxa, reported in term of either N/mm^2 or % within *Discoaster* Tan, 1927, are also reported. The dark and light grey shaded areas correspond to the CIE main excursion in-terval and CIE recovery interval, respectively. The dark grey band at the onset of the PETM marks the calcareous nannofossil dissolution interval (CNDI). BEE: benthic foraminiferal extinction event. After Agnini et al. (2014a).

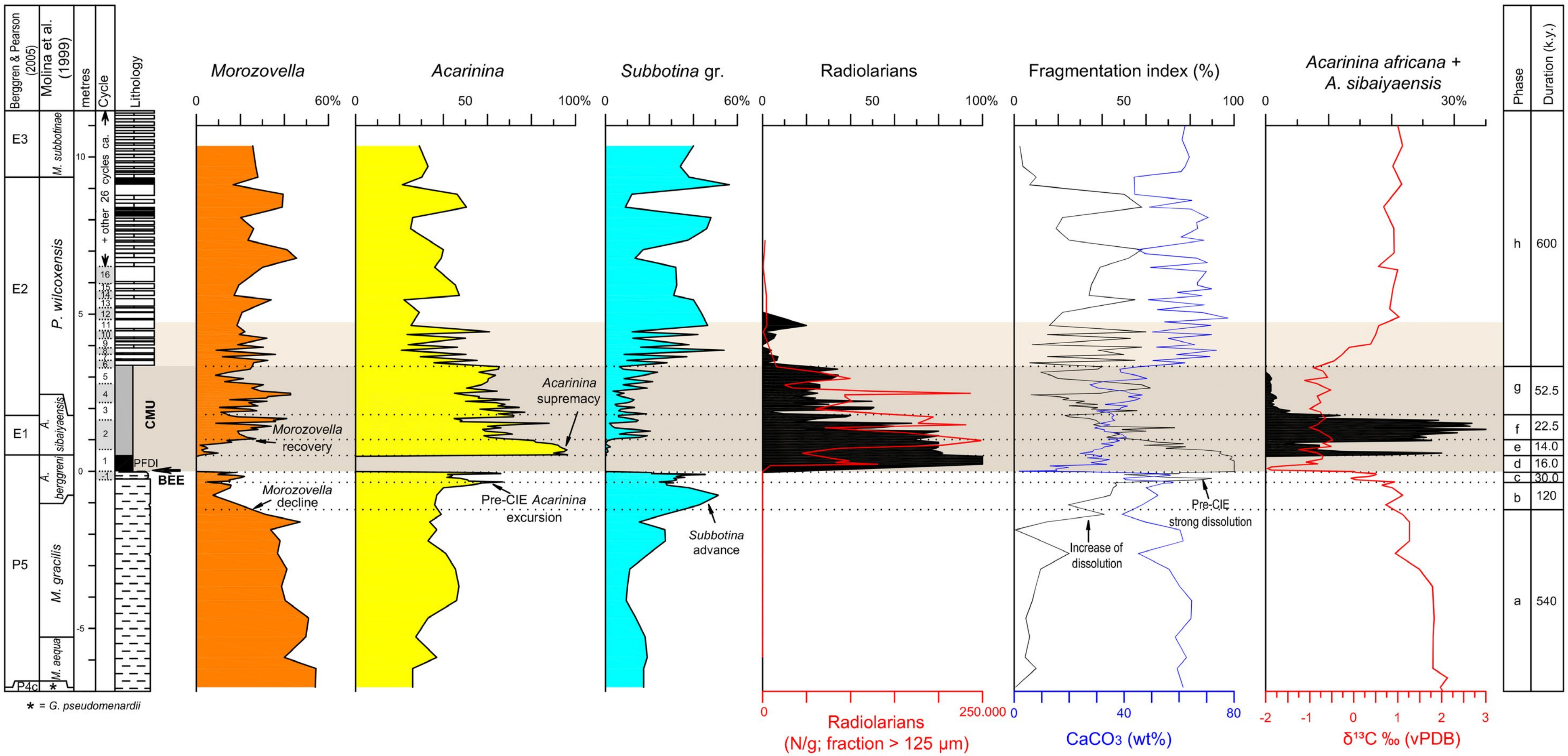

Fig. 8 - The planktic foraminiferal record at Forada section. Main changes in planktic foraminifera, radiolarians, fragmentation-index, $CaCO_3$, $\delta^{13}C$ across the PETM. Eight phases (a to h) have been identified on the basis of the prominent changes displayed by the components of assemblages. For the lithology see Luciani et al. (2007, fig. 2). Modified from Luciani et al. (2007).

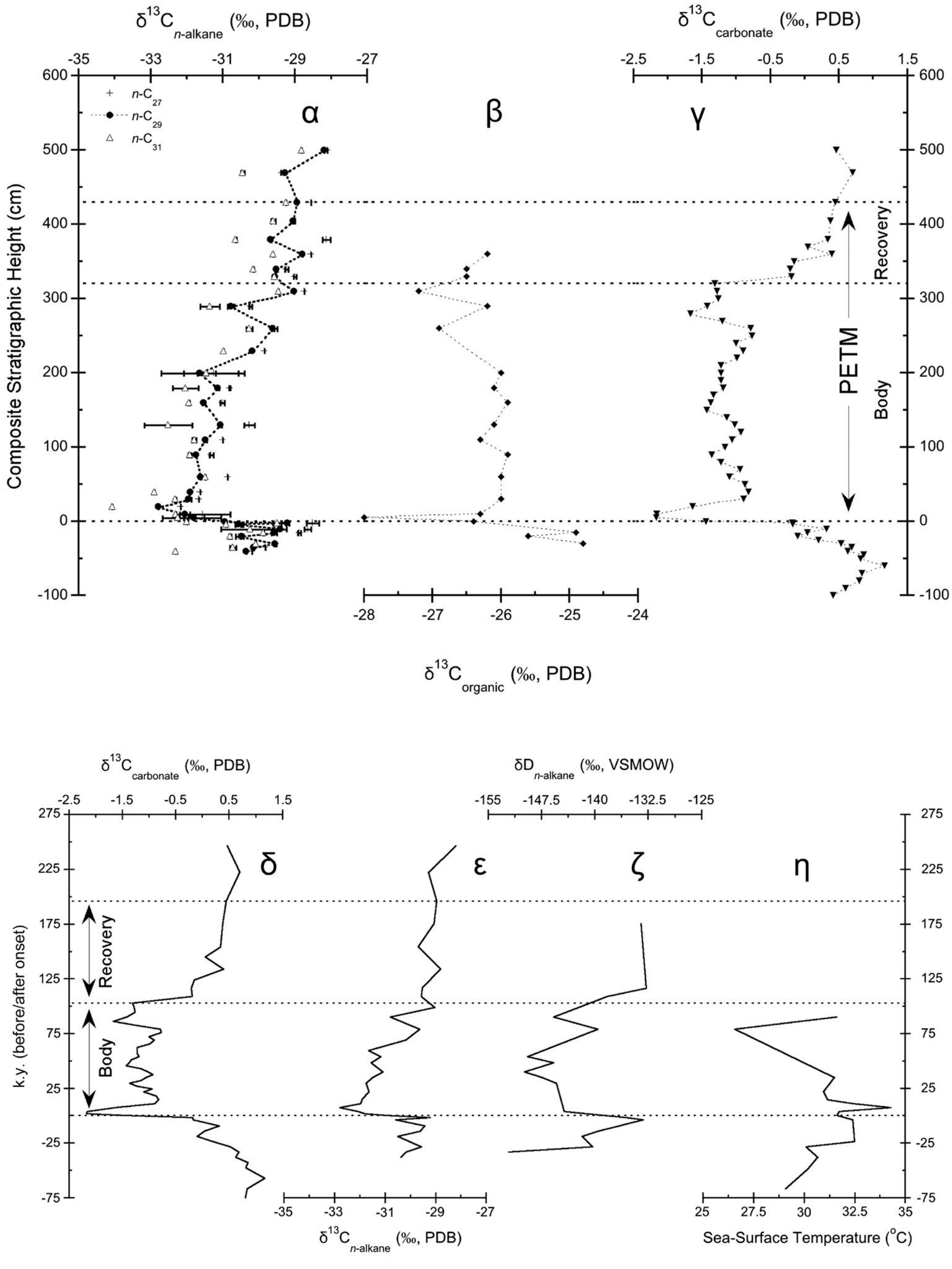

Fig. 9 - Upper row: stable carbon isotope ratios of higher plant n-alkanes (α), bulk organic carbon (β) and bulk carbonates (γ) across the Palaeocene/Eocene boundary interval at Forada section. Terrestrial higher plant n-C_{27}, n-C_{29}, and n-C_{31} $\delta^{13}C$ values are shown as crosses, closed circles, and triangles, respectively. Lower row: carbon isotope, hydrogen isotope, average chain length, and sea-surface temperature records from the Forada section relative to stratigraphic age. Bulk carbonate $\delta^{13}C$ values (δ), $\delta^{13}C$ (ε) and δD (ζ) values for n-C_{29}. Sea-surface temperature estimates from TEX_{86} (g). Modified after Tipple et al. (2011).

on the reinterpretation of original data of Lee & Odama (2009), Dallanave et al. (2012b) suggested that the PEMR might have simply been the result of a drilling-induced remagnetisation the analyzed sediment samples.

Marine and terrestrial records of carbon and hydrologic cycles variations during the PETM - Tipple et al. (2011) generated carbon isotope records from terrestrial biomarkers ($\delta^{13}C_{n\text{-alkane}}$), marine bulk carbonates ($\delta^{13}C_{carbonate}$), and bulk organic carbon ($\delta^{13}C_{organic}$) from the Forada section, in order to evaluate the mutual relationships between the hydrologic cycle, temperatures and terrestrial geochemical signatures (Fig. 9). For the very first time, this study allowed for a high-resolution estimate of the dynamics and changes in marine and terrestrial reservoirs within a single PETM section. At Forada, the terrestrial $\delta^{13}{}_{Cn\text{-alkane}}$ record lags behind the $\delta^{13}C_{carbonate}/\delta^{13}C_{organic}$ trend by ~4-5 k.y. at the onset of PETM, suggesting the incorporation of pre-PETM n-alkanes in sediments due to soil erosion, along with a residence time of soil-related n-alkanes of ca. 4000 years during the early CIE times. Hydrogen isotope records from higher-plant leaf waxes ($\delta D_{n\text{-alkane}}$) and sea-surface temperatures (SSTs) derived from TEX_{86} analyses were also established, in order to assess hydrologic and ocean temperature trends. TEX_{86}-derived SSTs show at first a

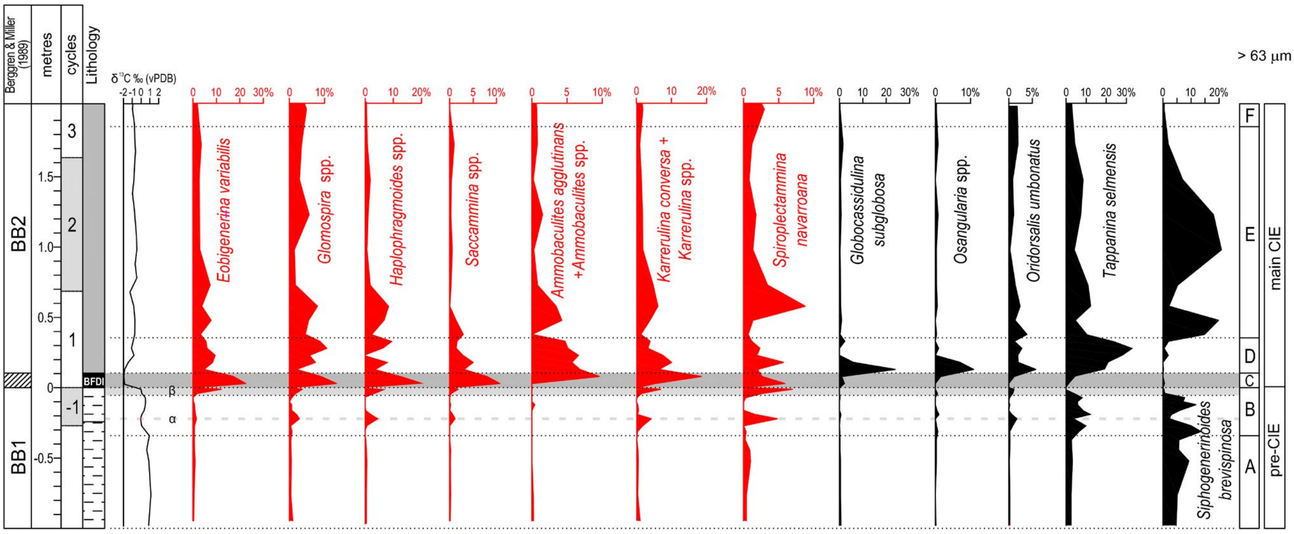

Fig. 10 - The Forada section. Enlargement of the interval from -1 to +2m across the Palaeocene/Eocene boundary showing the relative abundance of selected benthic foraminifera plotted against biostratigraphy, precessional cycles, lithology, $\delta^{13}C$ bulk record, recognised benthic foraminiferal assemblages (A to F) and isotopic intervals. Benthic foraminiferal biozonation after Berggren & Miller (1989). The grey bands indicate intervals of carbonate dissolution. α: pre-CIE dissolution interval; β: burndown layer; BFDI: benthic foraminiferal dissolution interval. Red: agglutinated taxa, black: hyaline taxa. After Giusberti et al. (2016).

gradual increase (3.5°C) right below the onset of the CIE, with peak values (ca. 35°C) that are attained at the base of the CIE (Fig. 9). The $\delta D_{n\text{-alkane}}$ record (Fig. 9) shows a shift to more positive values prior to the onset of the carbon isotope excursion, in parallel with SSTs, while lower $\delta D_{n\text{-alkane}}$ values are reported throughout the CMU. Tipple et al. (20111) concluded that both the hydrologic cycle and temperatures changed prior to the onset of the CIE, in parallel with changes in planktic foraminifera (i.e., acarininids bloom; Luciani et al., 2007), thus confirming a strong pre-event warming of the surface sea waters.

Towards an integration of Forada's PETM data sets - Giusberti et al. (2016) investigated the benthic foraminiferal record at Forada by coupling new and previously acquired data (Figs 10-11). Altogether, this work provided one of the most complete reconstruction available to date of the ecological and climatic changes that occurred across the PETM in the Tethyan area. About 34 k.y. before the CIE onset, both foraminiferal, molecular and geochemical data point to changing climatic and oceanographic conditions heralding the PETM (assemblage B; Figs 10-11). Such "PETM prelude", associated at Forada with a negative shift in bulk $\delta^{13}C$ previously evidenced by Luciani et al. (2007), is consistent with the results of various studies that reported on environmental changes prior to the onset of the CIE by some ten thousand years (e.g., Alegret et al., 2018 and references therein). The profound changes recorded at the onset of the PETM at Forada, as combined de-oxygenation, acidification and high environmental instability, and may have synergistically impacted the biota in deep-sea settings, thus leading to a massive benthic foraminiferal extinction over a time interval not longer than 4 k.y. (Giusberti et al., 2016). The first early Eocene benthic foraminiferal assemblages (C, D: ca. 12 k.y.; Fig. 11) at Forada show a complex succession of abundance peaks of agglutinated and calcareous recolonisers (Fig. 10). As confirmed by molecular and mineralogical proxies, these short-term turnovers point to increased precipitation and strong continental erosion during the early PETM, which ultimately led to a massive sediment discharge into the Belluno Basin. The strong precession-paced variability of biotic (i.e., foraminifera and radiolarians), mineralogical and molecular proxies in the overlying core CIE interval has been interpreted by Giusberti et al. (2016) as reflecting the alternation between wetter and drier periods (assemblages E and lower F; Fig. 11). This extreme climatic variability at the orbital time scale persisted, albeit with a declining intensity, well above the end of CIE recovery (middle and upper third of assemblage F). Weather extremes, persisting over several k.y., might have significantly increased the erosion rates and weathering on mainland by way of periods with alternating wet and dry conditions, which played a critical role in diminishing the atmospheric CO_2 levels (Giusberti et al., 2016). Information collected so far suggests that the Forada record, along with the comparable Zumaia record (Spain), holds a regionally-validated record of the climate dynamics, as well as the related responses of the sedimentary system at the continental margin, across the PETM (Dunkley Jones et al., 2018).

The Cicogna section

The Cicogna section, originally described by Di Napoli Alliata et al. (1970), is exposed continuously along the Cicogna Creek, about 14 km northeast of the Forada section (Fig. 4a). The section is ca. 80 m thick (Fig. 4c), and consists of 20 m of dominantly grey-greenish marls and marly limestones grading upwards to 60 m of reddish and greenish marls and marly limestones ("Marna della Vena d'Oro", an informal lithostratigraphic subunit of the Scaglia Rossa Formation; Fig. 4b). The succession is capped by the turbidites of the Belluno Flysch (Dallanave et al., 2009). The Cicogna section spans from the upper Palaeocene to the lower Eocene (CNP10-CNE4 calcareous

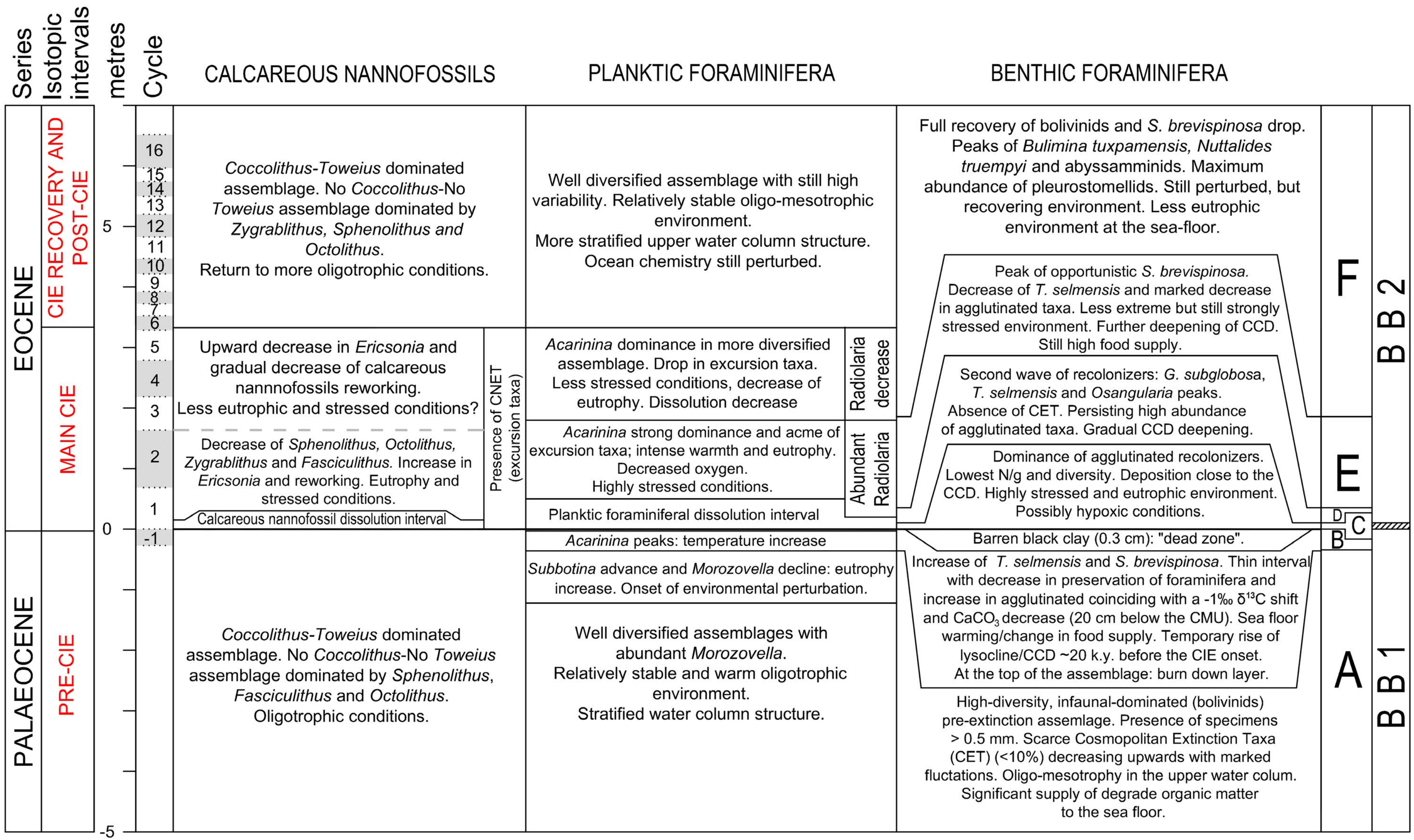

Fig. 11 - The Forada section. Synopsis of main calcareous plankton (calcareous nannofossils and planktic foraminifera) and benthic foraminiferal events and inferred environmental conditions, isotopic intervals, thickness, precessional cycles and benthic foraminiferal assemblages (A-F; see also Fig. 10). The stratigraphic intervals containing assemblages A and B, C, and D to F are considered as pre-extinction, extinction and repopulation intervals, respectively. Benthic foraminiferal zonation after Berggren and Miller (1989). CNET: calcareous nannofossil excursion taxa. After Giusberti et al. (2016).

nannofossil zones of Agnini et al., 2014; Fig. 4b). The interval between 28.7 m and 31.7 m consists of greenish and reddish clayey marls that have been attributed to the CMU (Dallanave et al., 2009). In its lower part (~40 cm), the CMU shows evidences of a modest tectonic disturbance (Krishan et al., 2015) that is problematic for high resolution studies of the early PETM.

Studies performed in the Cicogna section were especially aimed at refining the biomagnetostratigraphic record in the C25r-C24n interval (Dallanave et al., 2009). Furthermore, the relationships between changes in stable isotopes (i.e., the PETM and minor hyperthermals) and nannofossil assemblages were investigated, specifically by discriminating long-lasting and short-lived modifications within nannoliths, holococcoliths and placoliths (Agnini et al., 2016). Based on these results, Agnini et al. (2016) concluded that the PETM compelled the calcareous nannoplankton communities to undergo a rapid and profound evolution, which exerted permanent modifications on the overall taxonomic composition of the group. On the contrary, the less prominent hyperthermals that followed did not provide such dramatic effects, apart from lesser changes at the expense of a limited number of rare taxa that probably could not cope successfully with the climatic and environmental stress.

Dallanave et al. (2010) described two pronounced events of increasing detrital hematite located immediately above the Palaeocene/Eocene boundary in the Cicogna section, between ~54.9 and 54.6 Ma (PETM and post PETM interval), which were followed by a long-term increasing trend between ~54 Ma and ~52.2 Ma (Early Eocene Climatic Optimum). The authors speculated that the formation, transport, and deposition of massive hematite yields might have been promoted by periods of enhanced chemical weathering rates that most likely, as discussed above, were associated to the warm and humid conditions associated to the PETM and EECO events. Instead, Giusberti et al. (2016) postulated that the hematite peaks recorded in the proximal Forada section during the PETM were primarily indicative of a periodic variability in the amount of wind-blown dusts. In particular, the abundance of hematite in marine sediments would reflect the persistence of powerful high-pressure cells over the continent that, as a consequence, would ensure dry climates, with development of strong land-winds and massive conveyance of dust to the basin (Giusberti et al., 2016).

Krishan et al. (2015) reconstructed carbon and hydrogen isotopic records from leaf wax lipids for the Cicogna section, which were compared to the previous records obtained in the adjacent Forada section (Tipple et al., 2011) in order to gauge the intrabasinal variability and changes in the hydrological cycle at mid-latitudes during the PETM. Magnitude of the CIE anomaly in the Cicogna section (ca. -2.5 ‰) is smaller than that observed at Forada (ca. -3.5‰); this discrepancy was interpreted as the result of local mixing processes with older, pre-CIE ^{13}C-rich sources. A pre-event enrichment in ^{2}H was found at Forada, suggesting pre-PETM modifications of the hydrological cycle (Tipple et al., 2011). This isotopic event was not detected in the Cicogna record, probably because of the tectonic disturbance that affects the basal part of the PETM (see above). ^{2}H depletion in *n*-alkanes was detected in both sections within the CIE, which has been interpreted primary as a change in the isotopic composition of meteoric waters. This modification might result from a greater warming at lower latitudes, and/or an increased activity by extra-tropical convective storms (Krishan et al., 2015). The general δ^{2}H offset observed between the Forada and Cicogna sections throughout the interval of relevance may be explained in terms of different ^{2}H sources and/or topography, which may influence the local precipitation rates. Likewise, differences in compound distributions (average chain lengths, ACL) observed between the two localities suggest that the analyzed biomarkers may originate from different source areas. Altogether, Krishan et al. (2015) concluded that a most careful approach must be taken, when dealing with absolute magnitudes obtained from biomarkers in the attempt of reconstructing the zonal hydrological changes.

CONCLUSIONS

Information provided in the last decades by the Italian sections straddling the PETM offers critical insights on the climatic, biotic and environmental dynamics that took place in the Tethyan region during this dramatic event, included its onset and aftermaths. Although the Umbria-Marche and Veneto stratigraphic records can be correlated straightforwardly, each record allows for the reconstruction of vastly different scenarios. Specifically, the former is better comparable to the open ocean records, as being deposited in deep, pelagic environment with limited terrigenous input, while the latter deposited within a landlocked basin where the significant terrigenous input was paradigmatic of a more marginal marine setting. Considering that the documentation globally available is mainly represented by deep, open-ocean records, we deem that the stratigraphy preserved in the Veneto region provides a unique point of view on the manifold biotic and abiotic events that took place during the earliest Cenozoic.

ACKNOWLEDGEMENTS

The authors are deeply indebted to Domenico Rio for the original idea of the "Palaeogene Veneto Project", the financial, material and scientific support all over these years. Jacopo Amalfitano is warmly thanked for his support with graphics. We deeply thank Silvia Gardin, Nicoletta Mancin and Giorgio Carnevale for their constructive and valuable comments and suggestions.

REFERENCES

Agnini C., Capraro L., Giusberti L., Boscolo Galazzo F., Fornaciari E., Luciani V., Papazzoni C. & Rio D. (2014a). The Paleogene of the central-eastern Veneto Region (northeastern Italy). Climatic and Biotic Events of the Paleogene (CBEP) 2014. Post-conference field trip guidebook. July 5-6, 2014. 47 pp. Cooperativa Libraria Editrice Università di Padova, Padova.

Agnini C., Fornaciari E., Giusberti L., Backman J., Capraro L., Grandesso P., Luciani V., Muttoni G., Rio D. & Tateo F. (2005). The Early Paleogene of the Valbelluna (Venetian Southern Alps). Fieldtrip Guidebook ODP Leg 208 Post-Cruise Meeeting. 32 pp. Cooperativa Libraria Editrice Università di Padova (CLEUP), Padova.

Agnini C., Fornaciari E., Giusberti L., Grandesso P., Lanci L., Luciani V., Muttoni G., Palike H., Rio D., Spofforth D.J.A. & Stefani C. (2011). Integrated bio-magnetostratigraphy of the Alano section (NE Italy): a proposal for defining the Middle-Late Eocene boundary. *Geological Society of America Bulletin*, 123: 841-872.

Agnini C., Fornaciari E., Raffi I., Catanzariti R., Pälike H., Backman J. & Rio D. (2014b). Biozonation and biochronology of Paleogene calcareous nannofossils from low and middle latitudes. *Newsletters on Stratigraphy*, 47: 131-181.

Agnini C., Fornaciari E., Rio D., Tateo F., Backman J. & Giusberti L. (2007). Responses of calcareous nannofossil assemblages, mineralogy and geochemistry to the environmental perturbations across the Paleocene/Eocene boundary in the Venetian Pre-Alps. *Marine Micropaleontology*, 63: 19-38.

Agnini C., Macrì P., Backman J., Brinkhuis H., Fornaciari E., Giusberti L., Luciani V., Rio D. & Sluijs A. (2009). An early Eocene carbon cycle perturbation at ~52.5 Ma in the Southern Alps: Chronology and biotic response. *Paleoceanography*, 24: PA2209.

Agnini C., Muttoni G., Kent D.V. & Rio D. (2006). Eocene biostratigraphy and magnetic stratigraphy from Possagno, Italy: the calcareous nannofossil response to climate variability. *Earth and Planetary Science Letters*, 241: 815-830.

Agnini C., Spofforth D.J.A., Dickens G.R., Rio D., Pälike H., Backman J., Muttoni G. & Dallanave E. (2016). Stable isotope and calcareous nannofossil assemblage record of the late Paleocene and early Eocene (Cicogna section). *Climate of the Past*, 12: 883-909.

Alegret L., Ortiz N. & Molina E. (2009). Extinction and recovery of benthic foraminifera across the Paleocene-Eocene Thermal Maximum at the Alamedilla section (Southern Spain). *Palaeogeography, Palaeoclimatology, Palaeoecology*, 279: 186-200.

Alegret L., Reolid M. & Vega Pérez M. (2018). Environmental instability during the latest Paleocene at Zumaia (Basque-Cantabric Basin): The bellwether of the Paleocene-Eocene Thermal Maximum. *Palaeogeography, Palaeoclimatology, Palaeoecology*, 497: 186-200.

Alvarez W., Arthur M.A., Fischer A.G., Lowrie W., Napoleone G., Premoli Silva I. & Roggenthen W. (1977). Late Cretaceous–Paleocene geomagnetic reversal time scale: V. Type section in the pelagic limestone sequence at Gubbio, Italy. *Geological Society of America Bulletin*, 88: 383-389.

Alvarez W. & Montanari A. (1988). The Scaglia limestones (Late Cretaceous–Oligocene) in the northeastern Apennines carbonate sequence; stratigraphic context and geological significance. *In* Premoli Silva I., Coccioni R. & Montanari A. (eds), The Eocene–Oligocene Boundary in the Marche–Umbria Basin (Italy). International Subcommission on Paleogene Stratigraphy, Special Publication, Industrie Grafiche Fratelli Aniballi, Ancona: 13-29.

Angori E., Bernaola G. & Monechi S. (2007). Calcareous nannofossil assemblages and their response to the Paleocene-Eocene Thermal Maximum event at different latitudes: ODP Site 690 and Tethyan sections. *In* Monechi S., Coccioni R. & Rampino M.R. (eds), Large Ecosystem Perturbations: Causes and Consequences. *Geological Society of America Special Papers*, 424: 69-85.

Angori E. & Monechi S. (1996). High-resolution calcareous nannofossil biostratigraphy across the Paleocene/Eocene boundary at Caravaca (southern Spain). *In* Aubry M.-P. & Benjamini C. (eds), Paleocene/Eocene boundary events in space and time. *Israel Journal of Earth Sciences*, 44: 197-206.

Arenillas I., Molina E. & Schmitz B. (1999). Planktic foraminiferal and $\delta^{13}C$ isotopic changes across the Paleocene/Eocene boundary at Possagno (Italy). *International Journal of Earth Sciences*, 88: 352-364.

Arreguín-Rodríguez G.J., Alegret L., Sepúlveda J., Newman S. & Summons R.E. (2014). Enhanced terrestrial input supporting the *Glomospira* acme across the Paleocene-Eocene boundary in Southern Spain. *Micropaleontology*: 60, 43-51.

Aubry M.-P., Ouda K., Dupuis C., Berggren W.A., Van Couvering J.A., Ali J., Brinkhuis H., Gingerich P.R., Heilmann-Clausen C., Hooker J., Kent D.V., King C., Knox R.W.O.'B., Laga P., Molina E., Schmitz B., Steurbaut E. & Ward D.R. (2007). The Global Standard Stratotype-Section and Point (GSSP) for the base of the Eocene Series in the Dababiya section (Egypt). *Episodes*, 30: 271-286.

Berggren W.A., Kent D.V., Swisher III C.C. & Aubry M.-P. (1995). A revised Cenozoic geochronology and chronostratigraphy. *In* Berggren W.A., Kent D.V., Swisher III C.C., Aubry M.-P. & Hardenbol J. (eds), Geochronology, Time Scales and Global Stratigraphic Correlation. *SEPM Special Publication*: 54, 129-212.

Berggren W.A. & Miller K.G. (1989). Cenozoic bathyal and abyssal calcareous benthic foraminiferal zonation. *Micropaleontology*, 35: 308-320.

Berggren W.A. & Pearson P.N. (2005). A revised tropical to subtropical Paleogene planktonic foraminiferal zonation. *Journal of Foraminiferal Research*, 35: 279-298.

Black M. & Barnes B. (1959). The structure of Coccoliths from the English Chalk. *Geological Magazine*, 96: 321-328.

Bolli H.M. (1975). Monografia micropaleontogica sul Paleocene e l'Eocene di Possagno, Provincia di Treviso, Italia. *Schweizerische Paläontologische Abhandlungen*, 97: 1-22.

Boscolo Galazzo F., Giusberti L., Luciani V. & Thomas E. (2013). Paleoenvironmental changes during the Middle Eocene Climatic Optimum (MECO) and its aftermath: The benthic foraminiferal record from the Alano section (NE Italy). *Palaeogeography, Palaeoclimatology, Palaeoecology*, 378: 22-35.

Bowen G.J. & Zachos J.C. (2010). Rapid carbon sequestration at the termination of the Palaeocene-Eocene Thermal Maximum. *Nature Geoscience*, 3: 866-869.

Braga G., De Biase R., Grüning A. & Proto Decima F. (1975). Foraminiferi bentonici del Paleocene e dell'Eocene della sezione di Possagno. *In* Bolli H.M. (ed.), Monografia micropaleontogica sul Paleocene e l'Eocene di Possagno, Provincia di Treviso, Italia. *Schweizerische Paläontologische Abhandlungen*, 97: 85-111.

Bramlette M.N. & Sullivan F.R. (1961). Coccolithophorids and related Nannoplankton of the early Tertiary in California. *Micropaleontology*, 7: 129-188.

Bukry D. (1971). *Discoaster* evolutionary trends. *Micropaleontology*, 17: 43-52.

Bybell L.M. & Self-Trail J. (1995). Evolutionary, Biostratigraphic and Taxonomic Study of Calcareous Nannofossils from a Continuous Palaeocene-Eocene Boundary Section in New Jersey. *United States Geological Survey Professional Paper*, 1554: 1-36.

Canudo J.I., Keller G., Molina E. & Ortiz N. (1995). Planktic foraminiferal turnover and $\delta^{13}C$ isotopes across the Paleocene-Eocene transition at Caravaca and Zumaya, Spain. *Palaeogeography, Palaeoclimatology, Palaeoecology*, 114: 75-100.

Carmichael M.J., Inglis G.N., Badger M.P., Naafs B.D.A., Behrooz L., Remmelzwaal S., Monteiro F.M., Rohrssen M., Farnsworth A., Buss H.L., Dickson A.J., Valdes P.J., Lunt D.J. & Pancost R.D. (2017). Hydrological and associated biogeochemical consequences of rapid global warming during the Paleocene-Eocene Thermal Maximum. *Global and Planetary Change*, 157: 114-138.

Channell J.E.T., Bralower T.J. & Grandesso P. (1987). Biostratigraphic correlation of Mesozoic polarity chrons CM1 to CM23 at Capriolo and Xausa (Southern Alps, Italy). *Earth and Planetary Science Letters*, 85: 203-221.

Channell J.E.T., D'Argenio B. & Horvath F. (1979). Adria, the African promontory in Mesozoic Mediterranean palaeogeography. *Earth-Science Reviews*, 15: 231-292.

Channell J.E.T. & Grandesso P. (1987). A revised correlation of Mesozoic polarity chrons and calpionellid zones. *Earth Planetary Science Letters*, 85: 222-240.

Charisi S.D. & Schmitz B. (1995). Stable (δ^{13}C, δ^{18}O) and strontium (^{87}Sr/^{86}Sr) isotopes through the Paleocene at Gebel Aweina, eastern Tethyan region. *Palaeogeography, Palaeoclimatology, Palaeoecology*, 116: 103-129.

Coccioni R., Bancalà G., Catanzariti R., Fornaciari E., Frontalini F., Giusberti L., Jovane L., Luciani V., Savian J. & Sprovieri M. (2012). An integrated stratigraphic record of the Palaeocene–lower Eocene at Gubbio (Italy): New insights into the early Palaeogene hyperthermals and carbon isotope excursions. *Terra Nova*, 24: 380-386.

Coccioni R., Catanzariti R., Frontalini F., Galbrun B., Jovane L., Montanari A., Savian J.F. & Sideri M. (2016). Integrated magnetostratigraphy, biostratigraphy, and chronostratigraphy of the Paleogene pelagic succession at Gubbio (central Italy). *In* Menichetti M., Coccioni R. & Montanari A. (eds), The Stratigraphic Record of Gubbio: Integrated Stratigraphy of the Late Cretaceous–Paleogene Umbria-Marche Pelagic Basin. *Geological Society of America Special Papers*, 524: 139-160.

Coccioni R., Di Leo R., Galeotti S. & Monechi S. (1994). Integrated biostratigraphy and benthic foraminiferal faunal turnover across the Paleocene–Eocene boundary at Trabakua Pass section, Northern Spain. *Palaeopelagos*, 4: 87-100.

Coccioni R., Frontalini F., Bancalà G., Fornaciari E., Jovane L. & Sprovieri M. (2010). The Dan-C2 hyperthermal event at Gubbio (Italy): Global implications, environmental effects, and cause (s). *Earth and Planetary Science Letters*, 297: 298-305.

Coccioni R., Frontalini F., Catanzariti R., Jovane L., Rodelli D., Rodrigues I.M.M., Savian J.F., Giorgioni M. & Galbrun B. (2019). Paleoenvironmental signature of the Selandian-Thanetian Transition Event (STTE) and Early Late Paleocene Event (ELPE) in the Contessa Road section (western Neo-Tethys). *Palaeogeography, Palaeoclimatology, Palaeoecology*, 523: 62-77.

Coccioni R., Sideri M., Bancalà G., Catanzariti R., Frontalini F., Jovane L., Montanari A. & Savian J. (2013). Integrated stratigraphy (magneto-, bio-and chronostratigraphy) and geochronology of the Palaeogene pelagic succession of the Umbria-Marche Basin (central Italy). *In* Jovane L., Herrero-Barvera E., Hinnov L. & Housen B.A. (eds), Magnetic Methods and the Timing of Geological Processes. *Geological Society, London, Special Publication*, 373: 111-131.

Corfield R.M., Cartlidge J.E., Premoli Silva I. & Housley R.A. (1991). Oxygen and Carbon isotope stratigraphy of the Paleogene and Cretaceous limestones in the Bottaccione Gorge and the Contessa Highway sections, Umbria, Italy. *Terra Nova*, 3: 414-432.

Cushman J.A., 1939. New American Cretaceous Foraminifera. *Contributions from the Cushman Laboratory for Foraminiferal Research*, 15(4): 89-93.

Cramer B.S., Kent D.V. & Aubry M.-P. (2003). Orbital climate forcing of excursions in the late Paleocene–early Eocene (chrons C24n–C25n). *Paleoceanography*, 18: 1-25.

D'Ambrosia A.R., Clyde W.C., Fricke H.C., Gingerich P.D. & Abels H.A. (2017). Repetitive mammalian dwarfing during ancient greenhouse warming events. *Science Advances*, 3: e1601430

Dallanave E., Agnini C., Muttoni G. & Rio D. (2009). Magneto-biostratigraphy of the Cicogna section (Italy): implications for the late Paleocene-early Eocene time scale. *Earth and Planetary Science Letter*s, 285: 39-51.

Dallanave E., Agnini C., Muttoni G. & Rio D. (2012a). Paleocene magneto-biostratigraphy and climate-controlled rock magnetism from the Belluno Basin, Tethys Ocean, Italy. *Palaeogeography*, *Palaeoclimatology*, *Palaeoecology*, 337-338: 130-142.

Dallanave E., Muttoni G., Agnini C., Tauxe L. & Rio D. (2012b). Is there a normal magnetic polarity event during the Paleocene–Eocene thermal maximum (~55 Ma)? The paleomagnetic record of the Belluno Basin (Italy). *Geophysical Journal International*, 191: 517-529.

Dallanave E., Tauxe L., Muttoni G. & Rio D. (2010). Silicate weathering machine at work: Rock magnetic data from the late Paleocene-early Eocene Cicogna section, Italy. *Geochemistry Geophysics Geosystems*, 11: Q07008.

DeConto R.M., Galeotti S., Pagani M., Tracy D., Schaefer K., Zhang T., Pollard D. & Beerling D.J. (2012). Past extreme warming events linked to massive carbon release from thawing permafrost. *Nature*, 484: 87-91.

Deflandre G. (1952). Classe des Coccolithophoridés. (Coccolithophoridae. Lohmann, 1902). *In* Grassé P.P. (ed.), Traité de Zoologie, Masson, Paris: 439-470.

Deflandre G. (1959). Sur les nannofossiles calcaires et leur systématique. *Revue de Micropaleontologie*, 2: 127-152.

D'Onofrio R., Luciani V., Fornaciari E., Giusberti L., Boscolo Galazzo F., Dallanave E., Westerhold T., Sprovieri M. & Telch S. (2016). Environmental perturbations at the early Eocene ETM2, H2, and 11 events as inferred by Tethyan calcareous plankton (Terche section, northeastern Italy). *Paleoceanography*, 31: 1225-1247.

Di Napoli Alliata E., Proto Decima F. & Pellegrini G.B. (1970). Studio Geologico, Stratigrafico e Micropaleontologico dei Dintorni di Belluno. *Memorie della Società Geologica Italiana*, 9: 1-28.

Dunkley Jones T., Manners H.R., Hoggett M., Kirtland Turner S.K., Westerhold T., Leng M.J., Pancost R.D., Ridgwell A., Alegret L., Duller R. & Grimes S.T. (2018). Dynamics of sediment flux to a bathyal continental margin section through the Paleocene–Eocene Thermal Maximum. *Climate of the Past*, 14: 1035-1049.

Egger H., Homayoun M., Huber H., Rögl F. & Schmitz B. (2005). Early Eocene climatic, volcanic, and biotic events in the northwestern Tethyan Untersberg section, Austria. *Palaeogeography, Palaeoclimatology, Palaeoecology*, 217: 243-264.

El-Naggar Z.R. (1966). Stratigraphy and planktonic foraminifera of the Upper Cretaceous-Lower Tertiary succession in the Esna-Idfu region, Nile Valley, Egypt, U.A.R. *Bulletin of the British Museum* (*Natural History*) *Geology*, supplement, 2: 1-291.

Ernst S.R., Guasti E., Dupuis C. & Speijer R.P. (2006). Environmental perturbation in the southern Tethys across the Paleocene/Eocene boundary (Dababyia, Egypt): foraminiferal and clay minerals record. *Marine Micropaleontology*, 60: 89-111.

Fabiani R. (1915). Il Paleogene del Veneto. *Memorie dell'Istituto di Geologia della Regia Università di Padova,* 3: 1-336.

Fornaciari E., Giusberti L., Luciani V., Tateo F., Agnini C., Backman J., Oddone M. & Rio D. (2007). An expanded Cretaceous-Tertiary transition in a pelagic setting of the Southern Alps (central-western Tethys). *Palaeogeography, Palaeoclimatology, Palaeoecology*, 255: 98-131.

Foster G.L., Hull P., Lunt D.J. & Zachos J.C. (2018). Placing our current 'hyperthermal' in the context of rapid climate change in our geological past. *Philosophical Transactions of the Royal Society*, A 376: 20170086.

Frieling J., Svensen H.H., Planke S., Cramwinckel M.J, Selnes H. & Sluijs A. (2016). Thermogenic methane release as a cause for the long duration of the PETM. *PNAS*, 113: 12059-12064.

Frontalini F., Coccioni R., Catanzariti R., Jovane L., Savian J. F. & Sprovieri M. (2016). The Eocene Thermal Maximum 3: Reading the environmental perturbations at Gubbio (Italy). *In* Menichetti M., Coccioni R. & Montanari A. (eds), The Stratigraphic Record of Gubbio: Integrated Stratigraphy of the Late Cretaceous–Paleogene Umbria-Marche Pelagic Basin. *Geological Society of America Special Papers*, 524: 161-175.

Galeotti S., Angori E., Coccioni R., Ferrari G., Galbrun B., Monechi S., Premoli Silva I., Speijer R.P. & Turi B. (2000). Integrated stratigraphy across the Paleocene/Eocene boundary in the Contessa Road section, Gubbio (central Italy). *Bulletin de la Société Géologique de France,* 171: 355-365.

Galeotti S., Kaminski M.A., Coccioni R. & Speijer R. (2004). High resolution deep water agglutinated foraminiferal record across the Paleocene/Eocene transition in the Contessa Road Section (central Italy). *In* Bubik M. & Kaminski M.A. (eds), Proceedings of the Sixth International Workshop on

Agglutinated Foraminifera. *Grzybowski Foundation Special Publication*, 8: 83-103.
Galeotti S., Krishnan S., Pagani M., Lanci L., Gaudio A., Zachos J.C., Monechi S., Morelli G. & Lourens L. (2010). Orbital chronology of early Eocene hyperthermals from the Contessa Road section, central Italy. *Earth and Planetary Science Letters*, 290: 192-200.
Galeotti S., Moretti M., Sabatino N., Sprovieri M., Ceccatelli M., Francescone F., Lanci L., Lauretano V. & Monechi S. (2017). Cyclochronology of the Early Eocene carbon isotope record from a composite Contessa Road-Bottaccione section (Gubbio, central Italy). *Newsletters on Stratigraphy*, 50: 231-244.
Gingerich P.D. (2003). Mammalian response to climate change at the Paleocene-Eocene boundary: Polecat Bench record in the northern Bighorn Basin, Wyoming. *In* Wing S.L., Gingerich P.D., Schmitz B. & Thomas E. (eds), Causes and Consequences of Globally Warm Climates in the Early Paleogene. *Geological Society of America Special Papers*, 369: 463-478.
Gingerich P. D. (2006). Environment and evolution through the Paleocene–Eocene thermal maximum. *Trends in Ecology & Evolution*, 21: 246-253.
Giusberti L., Bannikov A., Boscolo Galazzo F., Fornaciari E., Frieling J., Luciani V., Papazzoni C.A., Roghi G., Schouten S., Sluijs A., Bosellini F.R. & Zorzin R. (2014). A new *Fossil-Lagerstätte* from the Lower Eocene of Lessini Mountains (northern Italy): A multidisciplinary approach. *Palaeogeography, Palaeoclimatology, Palaeoecology*, 403: 1-15.
Giusberti L., Boscolo Galazzo F. & Thomas E. (2016). Variability in climate and productivity during the Paleocene–Eocene Thermal Maximum in the western Tethys (Forada section). *Climate of the Past*, 12: 213-240.
Giusberti L., Coccioni R., Sprovieri M. & Tateo F. (2009). Perturbation at the sea floor during the Paleocene-Eocene Thermal Maximum: evidence from benthic foraminifera at Contessa Road, Italy. *Marine Micropaleontology*, 70: 102-119.
Giusberti L., Kaminski M.A. & Mancin N. (2018). The bathyal larger lituolid *Neonavarella* n. gen. (Foraminifera) from the Thanetian Scaglia Rossa Formation of northeastern Italy. *Micropaleontology*, 64: 417-434.
Giusberti L., Rio D., Agnini C., Backman J., Fornaciari E., Tateo F. & Oddone M. (2007). Mode and tempo of the Paleocene-Eocene thermal maximum in an expanded section from the Venetian pre-Alps. *Geological Society of America Bullettin*, 119: 391-412.
Gradstein F.M., Ogg J.G., Schmitz M.D. & Ogg G.M. (2012). A Geologic Time Scale 2012. 1144 pp. Elsevier, Boston.
Grzybowski J. (1898). Otwornice pokładów naftonośnych okolicy Krosna-Foraminifera of oil-bearing strata in the neighbourhood of Krosno. *Rozprawy Wydziału Matematyczno-Przyrodniczego Akademii Umiejętności*, 33: 257-305.
Gutjahr M., Ridgwell A., Sexton P.F., Anagnostou E., Pearson P.N., Pälike H., Norris R.D., Thomas E. & Foster G.L. (2017). Very large release of mostly volcanic carbon during the Palaeocene–Eocene Thermal Maximum. *Nature*, 548: 573-577.
Hay W.W. & Mohler H.P. (1967). Calcareous nannoplankton from Early Tertiary rocks at Point Labau, France and Paleocene-Early Eocene correlations. *Journal of Paleontology*, 41: 1505-1541.
Jones T.R. & Parker W.K. (1860). On the Rhizopodal fauna of the Mediterranean, compared with that of the Italian and some other Tertiary deposits. *Quarterly Journal of the Geological Society*, 16: 292-307.
Jovane L., Florindo F., Coccioni R., Dinarès-Turell J., Marsili A., Monechi S., Roberts A.P. & Sprovieri M. (2007). The middle Eocene climatic optimum event in the Contessa Highway section, Umbrian Apennines, Italy. *Geological Society of America Bulletin*, 119: 413-427.
Kahn A. & Aubry M.-P. (2004). Provincialism associated with the Paleocene/Eocene ther-mal maximum: temporal constraint. *Marine Micropaleontology*, 52: 117-131.
Kennett J.P. & Stott L.D. (1990). Proteus and Proto-Oceanus: ancestral Paleogene Oceans as revealed from Antarctic stable isotopic results; ODP Leg 113. *Proceedings of the Ocean Drilling Program, Scientific Results*, 113: 865-880.
Kennett J.P. & Stott L.D. (1991). Abrupt deep-sea warming, palaeoceanographic changes and benthic extinctions at the end of the Palaeocene. *Nature*, 353: 225-229.
Koch P.L., Zachos J.C. & Gingerich P.D. (1992). Correlation between isotope records in marine and continental carbon reservoirs near the Palaeocene/Eocene boundary. *Nature*, 358: 319-322.
Krishnan S., Pagani M. & Agnini C. (2015). Leaf waxes as recorders of paleoclimatic changes during the Paleocene-Eocene Thermal Maximum: Regional expressions from the Belluno Basin. *Organic Geochemistry*, 80: 8-17.
Lee Y.S. & Kodama K. (2009). A possible link between the geomagnetic field and catastrophic climate at the Paleocene–Eocene thermal maximum. *Geology*, 37: 1047-1050.
Lowrie W., Alvarez A., Napoleone G., Perch-Nielsen K., Premoli Silva I. & Toumarkine M. (1982). Paleogene magnetic stratigraphy in the Umbrian pelagic carbonate rocks: The Contessa sections, Gubbio. *Geological Society of America Bulletin*, 93: 414-432.
Lu G., Keller G., Adatte T., Ortiz N. & Molina E. (1996). Long-term (105) or short-term (103) excursion near the Paleocene-Eocene transition: evidence from the Tethys. *Terra Nova*, 8: 347-355.
Luciani V., Dickens J., Backman J., Fornaciari E., Giusberti L., Agnini C. & D'Onofrio R. (2016). Major perturbations in the global carbon cycle and photosymbiont-bearing planktic foraminifera during the early Eocene. *Climate of the Past*, 12: 981-1007.
Luciani V. & Giusberti L. (2014). Reassessment of the early-middle Eocene planktic foraminiferal biomagnetochronology: New evidence from the Tethyan Possagno section (NE Italy) and western North Atlantic Ocean ODP Site 1051. *Journal of Foraminiferal Research*, 44: 187-201.
Luciani V., Giusberti L., Agnini C., Backman J., Fornaciari E. & Rio D. (2007). The Paleocene-Eocene Thermal Maximum as recorded by Tethyan planktonic foraminifera in the Forada section (northern Italy). *Marine Micropaleontology*, 64: 189-214.
Luterbacher H.P. (1964). Studies in some *Globorotalia* from the Paleocene and lower Eocene of Central Apennines. *Eclogae Geologicae Helvetiae*, 57: 631-730.
Luterbacher H.P. & Premoli-Silva I. (1964). Biostratigrafia del limite Cretaceo–Terziario nell'Appennino centrale. *Rivista Italiana di Paleontologia e Stratigrafia*, 70: 67-128.
Marie P. (1956). Sur quelques foraminifères nouveaux du Crétacé supérieur belge. *Annales de la Société géologique de Belgique*, 80: B235-B257.
Marramà G., Bannikov A.B., Tyler J.C., Zorzin R. & Carnevale G. (2016). Controlled excavations in the Pesciara and Monte Postale sites provide new insights about the palaeoecology and taphonomy of the fish assemblages of the Eocene Bolca Konservat-Lagerstätte, Italy. *Palaeogeography, Palaeoclimatology, Palaeoecology*, 454: 228-245.
Martini E. (1971). Standard Tertiary and Quaternary calcareous nannoplankton zonation. *In* Farinacci A. (ed.), Proceedings of the 2nd International Conference on Planktonic Microfossils, 2: 739-785.
McInerney F.A. & Wing S.L. (2011). The Paleocene-Eocene thermal maximum: A perturbation of carbon cycle, climate, and biosphere with implications for the future. *Annual Review of Earth and Planetary Sciences*, 39: 489-516.
Molina E., Canudo J.I., Martínez-Ruiz F. & Ortiz N. (1994). Integrated stratigraphy across the Paleocene/Eocene boundary at Caravaca, southern Spain. *Eclogae geologicae Helvetiae*, 87: 47-61.
Monechi S. & Pirini Radrizzani C. (1975). Nannoplankton from Scaglia Umbra Formation (Gubbio) at Cretaceous-Tertiary boundary. *Rivista Italiana di Paleontologia e Stratigrafia*, 81: 31-44.

Monechi S. & Thierstein H.R. (1985). Late Cretaceous-Eocene nannofossil and magnetostratigraphic correlations near Gubbio, Italy. *Marine Micropaleontology*, 9: 419-440.
Murphy B.H., Farley K.A. & Zachos J.C. (2010). An extraterrestrial ^{3}He-based timescale for the Paleocene-Eocene thermal maximum (PETM) from Walvis Ridge, IODP Site 1266. *Geochimica et Cosmochimica Acta*, 74: 5098-5108.
Napoleone G., Premoli Silva I., Heller F., Cheli P., Corezzi S. & Fischer A.G. (1983). Eocene magnetic stratigraphy at Gubbio, Italy, and its implications for Paleogene geochronology. *Geological Society of America Bulletin*, 94: 181-191.
Okada H. & Bukry D. (1980). Supplementary modification and introduction of code numbers to the low-latitude coccolith biostratigraphic zonation (Bukry 1973, 1975). *Marine Micropaleontology*, 5: 321-325.
Ortiz N. (1995). Differential patterns of benthic foraminiferal extinctions near the Paleocene/Eocene boundary in the North Atlantic and the western Tethys. *Marine Micropaleontology*: 26, 341-359.
Papazzoni C.A., Fornaciari E., Giusberti L., Vescogni A. & Fornaciari B. (2017). Integrating Shallow Benthic and Calcareous Nannofossil Zones: the lower Eocene of the Monte Postale section (Northern Italy). *Palaios*, 32: 6-17.
Poletti I., Premoli Silva I., Masetti D., Pipan M. & Claps M. (2004). Orbitally driven fertility cycles in the Palaeocene pelagic sequences of the Southern Alps (Northern Italy). *Sedimentary Geology*, 164: 35-54.
Pujalte V., Baceta J.I. & Schmitz B. (2015). A massive input of coarse-grained siliciclastics in the Pyrenean Basin during the PETM: the missing ingredient in a coeval abrupt change in hydrological regime. *Climate of the Past*, 11: 1653-1672.
Raffi I. & De Bernardi B. (2008). Response of calcareous nannofossils to the Paleocene–Eocene Thermal Maximum: observations on composition, preservation and calcification in sediments from ODP Site 1263 (Walvis Ridge-SW Atlantic). *Marine Micropaleontology*, 69: 119-138.
Renz O. (1936). Stratigraphische und mikropaleontologische Untersuchung der Scaglia (Obere Kreid-Tertiär) im zentralen Apennin. *Eclogae geologicae Helvetiae*, 29: 1-149.
Rio D., Premoli Silva I. & Capraro L. (2003). The Geologic Time Scale and the Italian stratigraphic record. *Episodes*, 26: 259-263.
Röhl U., Westerhold T., Bralower T.J. & Zachos J.C. (2007). On the duration of the Paleocene-Eocene Thermal Maximum (PETM). *Geochemistry Geophysics Geosystems*, 8: 12002.
Romein A.J.T. (1979). Lineages in Early Paleogene calcareous nannoplankton. *Utrecht Micropaleontological Bulletins*, 22: 1-231.
Schaller M.F. & Fung M.K. (2018). The terrestrial impact evidence at the Paleocene-Eocene boundary and sequence of environmental change on the continental shelf. *Philosophical Transactions of the Royal Society A*, 376: 20170081.
Schmitz B., Pujalte V. & Núñez-Betelu K. (2001). Climate and sea-level perturbations during the initial Eocene thermal maximum: Evidence from siliciclastic units in the Basque Basin (Ermua, Zumaia and Trabakua Pass), northern Spain. *Palaeogeography, Palaeoclimatology, Palaeoecology*, 165: 299-320.
Schwarz E.H.L. (1894). Coccoliths. *Annals and Magazine of Natural History*, 14: 341-346.
Sluijs A., Bowen G.J., Brinkhuis H., Lourens L.J. & Thomas E. (2007). The Palaeocene-Eocene Thermal Maximum super greenhouse: Biotic and geochemical signatures, age models and mechanisms of global change. *In* Williams M., Hayward A., Gregory J. & Schmidt D.N. (eds), Deep Time Perspectives on Climate Change: Marrying the Signal from Computer Models and Biological Proxies. *The Micropalaeontological Society, Special Publications*, Geological Society, London: 323-349.
Speijer R.P. (1994). Extinction and recovery patterns in benthic foraminiferal paleocommunities across the Cretaceous/Paleogene and Paleocene/Eocene boundaries. *Geologica Ultraiectina*, 124: 77-90.
Speijer R.P., Scheibner C., Stassen P. & Morsi, A.-M. (2012). Response of marine ecosystems to deep-time global warming: a synthesis of biotic patterns across the Paleocene-Eocene thermal maximum (PETM). *Austrian Journal of Earth Sciences*, 105: 6-16.
Speijer R.P., Schmitz B., Aubry M.-P. & Charisi S.D. (1996). The latest Paleocene benthic extinction event: punctuated turnover in outer neritic foraminiferal faunas from Gebel Aweina, Egypt. In Aubry M.-P. & Benjamini C. (eds), Paleocene/Eocene boundary events in space and time. *Israel Journal of Earth Sciences*, 44: 207-222.
Tan S.H. (1927). Discoasteridae incertae sedis. *Proceedings of the Koninklijke Nederlandse Akademie van Wetenschappen, Section of Sciences*, 30: 411-419.
Thomas E. (1998). Biogeography of the late Paleocene benthic foraminiferal extinction. *In* Aubry M.P., Lucas S. & Berggren W.A. (eds), Late Paleocene-Early Eocene Climatic and Biotic Events in the Marine and Terrestrial Records. Columbia University Press, New York: 214-243.
Thomas E. (2007). Cenozoic mass extinctions in the deep sea: what perturbs the largest habitat on Earth? *In* Monechi S., Coccioni R. & Rampino M.R. (eds), Large Ecosystem Perturbations: Causes and Consequences. *Geological Society of America Special Papers*, 424: 1-23.
Tipple B., Pagani M., Krishnan S., Dirghang S.S., Galeotti S., Agnini C., Giusberti L. & Rio D. (2011). Coupled high-resolution marine and terrestrial records of carbon and hydrologic cycles variations during the Paleocene-Eocene Thermal Maximum (PETM). *Earth and Planetary Science Letters*, 311: 82-92.
Turner S.K. (2018). Constraints on the onset duration of the Paleocene–Eocene Thermal Maximum. *Philosophical Transactions of the Royal Society A*, 376: 20170082.
Wade B.S., Pearson P.N., Berggren W.A. & Pälike H. (2011). Review and revision of Cenozoic tropical planktonic foraminiferal biostratigraphy and calibration to the geomagnetic polarity and astronomical time scale. *Earth-Science Reviews*: 104, 111-142.
Zachos J.C., Lohmann K.C., Walker J.C.G. & Wise S.W. (1993). Abrupt climate change and transient climates during the Paleogene: a marine perspective. *The Journal of Geology*, 101: 191-213.
Zachos J.C., Pagani M., Sloan L.C., Thomas E. & Billups K. (2001). Trends, rhythms, and aberrations in global climate 65 Ma to present. *Science*, 292: 686-693.
Zachos J.C., Röhl U., Schellenberg S.A., Sluijs A., Hodell D.A., Kelly D.C., Thomas E., Nicolo M., Raffi I., Lourens L.J., McCarren H. & Kroon D. (2005). Rapid acidification of the ocean during the Paleocene-Eocene thermal maximum. *Science*, 308: 1611-1615.

Manuscript received 1 March 2019
Revised manuscript accepted 1 April 2019
Published online 30 April 2019
Guest Editors Massimo Bernardi & Giorgio Carnevale